Article

Mechanistic Studies on the Binding of Nitric Oxide to a Synthetic Heme–Thiolate Complex Relevant to Cytochrome P450

Alicja Franke, Grayna Stochel, Noriyuki Suzuki, Tsunehiko Higuchi, Kimiko Okuzono, and Rudi van Eldik

J. Am. Chem. Soc., **2005**, 127 (15), 5360-5375• DOI: 10.1021/ja047572u • Publication Date (Web): 25 March 2005

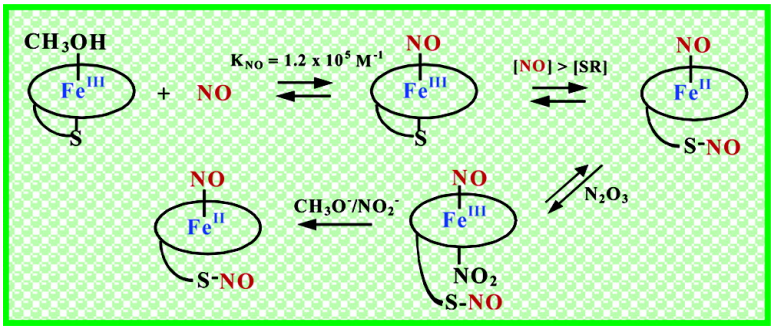

More About This Article

Additional resources and features associated with this article are available within the HTML version:

- Supporting Information
- Links to the 6 articles that cite this article, as of the time of this article download
- Access to high resolution figures
- Links to articles and content related to this article
- Copyright permission to reproduce figures and/or text from this article

View the Full Text HTML

J|A|C|S
ARTICLES
Published on Web 03/25/2005

Mechanistic Studies on the Binding of Nitric Oxide to a Synthetic Heme−Thiolate Complex Relevant to Cytochrome P450

Alicja Franke,[†] Grażyna Stochel,[‡] Noriyuki Suzuki,[§] Tsunehiko Higuchi,[¶] Kimiko Okuzono,[¶] and Rudi van Eldik*,[†]

Contribution from the Institute for Inorganic Chemistry, University of Erlangen-Nürnberg, Egerlandstrasse 1, 91058 Erlangen, Germany, Faculty of Chemistry, Jagiellonian University, Ingardena 3, Kraków 30060, Poland, Graduate School of Pharmaceutical Sciences, The University of Tokyo, 7-3-1 Hongo, Bunkyo-ku, Tokyo 113-0033, Japan, and Graduate School of Pharmaceutical Sciences, Nagoya City University, 3-1 Tanabe-dori, Mizuho-ku, Nagoya 467-8603, Japan

Received April 27, 2004; Revised Manuscript Received February 14, 2005; E-mail: vaneldik@chemie.uni-erlangen.de

Abstract: The synthetic heme−thiolate complex (SR) in methanol binds nitric oxide ($k_{on} = (2.7 \pm 0.2) \times 10^6$ M^{-1} s^{-1} at 25 °C) to form SR(NO). The binding of NO to the SR complex in a noncoordinating solvent, such as toluene, was found to be almost 3 orders of magnitude faster than that in methanol. The activation parameters $\Delta H^{\ddagger}$, $\Delta S^{\ddagger}$, and $\Delta V^{\ddagger}$ for the formation of SR(NO) in methanol are consistent with the operation of a limiting dissociative mechanism, dominated by dissociation of methanol in SR(MeOH). In the presence of an excess of NO, the formation of SR(NO) is followed by subsequent slower reactions. The substantially negative activation entropy and activation volume values found for the second observed reaction step support an associative mechanism which involves attack of a second NO molecule on the thiolate ligand in the initially formed SR(NO) complex. The following slower reactions are strongly accelerated by a large excess of NO or by the presence of NO_2^- in the SR/NO reaction mixture. They can be accounted for in terms of dynamic equilibria between higher nitrogen oxides (NO_x) and reactive SR species, which lead to the formation of a nitrosyl−nitrite complex of SR(Fe^{II}) as the final product. This finding is clearly supported by laser flash photolysis studies on the SR/NO reaction mixture, which do not reveal simple NO photolabilization from SR(Fe^{III})(NO), but rather involve the generation of at least three photoinduced intermediates decaying with different rate constants to the starting material. The species formed along the proposed reaction pathways were characterized by FTIR and EPR spectroscopy. The results are discussed in terms of their relevance for the biological function of cytochrome P450 enzymes and in context of results for the reaction of NO with imidazole- and thiolate-ligated iron(III) hemoproteins.

Introduction

Nitric oxide (NO) fulfills important roles in mammalian biology as an intracellular signaling agent for a variety of biological functions, such as vasodilation, neurotransmission, bronchodilation, and cytotoxic immune response.[1] Much of the biochemistry of this molecule involves heme proteins, including the biosynthesis of nitric oxide and signal transduction mediated by NO.[2] In this context, recent studies have been concerned with the preparation and mechanistic evaluation of synthetic iron(III/II) porphyrin complexes as useful biomimetic model systems in simulating the mechanism of heme ligand binding and activation and, thereby, determining the distinctive features of the active site of heme proteins.[3] Of significant interest is the high reactivity of model porphyrins coupled to the ability to undergo fast ligand substitution and redox cycling.[4−7] While the NO binding to heme−imidazole complexes has been the subject of many investigations,[8−10] fewer studies have been carried out with synthetic NO−heme−thiolate adducts, in part, because the thiolate-coordinated heme models tend to be

[†] University of Erlangen-Nürnberg.
[‡] Jagiellonian University.
[§] The University of Tokyo.
[¶] Nagoya City University.

(1) (a) Palmer, R. M. J.; Ferrige, A. G.; Moncada, S. *Nature* **1987**, *327*, 524. (b) Moncada, S.; Palmer, R. M. J.; Higgs, E. A. *Pharmacol. Rev.* **1991**, *43*, 109. (c) Feelisch, M.; Stamler, J. S. *Methods in Nitric Oxide Research*; John Wiley and Sons: Chichester, England, 1996; see references therein.
(2) (a) Traylor, T. G.; Sharma, V. S. *Biochemistry* **1992**, *31*, 2847. (b) Burstyn, J. N.; Yu, A. E.; Dierks, E. A.; Hawkins, B. K.; Dawson, J. H. *Biochemistry* **1995**, *34*, 5896.
(3) (a) Hong, A. P.; Bahnemann, D. W.; Hoffman, M. R. *J. Phys. Chem.* **1987**, *91*, 6245. (b) Meunier, B *Chem. Rev.* **1992**, *92*, 1411. (c) Behra, G.; Sigg, L. *Nature* **1990**, *344*, 419.
(4) (a) Lavallee, D. K. *Coord. Chem. Rev.* **1985**, *61*, 55. (b) Hoshino, M.; Lavermann, L.; Ford, P. C. *Coord. Chem. Rev.* **1999**, *187*, 75 and references therein.
(5) Ostrich, I. J.; Liu, G.; Dodgen, H. W.; Hunt, J. P. *Inorg. Chem.* **1980**, *19*, 619.
(6) Swaddle, T. W.; Merbach, A. E. *Inorg. Chem.* **1981**, *20*, 4212.
(7) Schneppensieper, T.; Zahl, A.; van Eldik, R. *Angew. Chem., Int. Ed.* **2001**, *40*, 1678.
(8) Zhao, Y.; Hoganson, C.; Babcock, G. T.; Marletta, M. A. *Biochemistry* **1998**, *37*, 12458.
(9) Tyryshkin, A. M.; Dikanov, S. A.; Reijerse, E. J.; Burgard, C.; Hütterman, J. *J. Am. Chem. Soc.* **1999**, *121*, 3396.
(10) Rich, A. M.; Armstrong, R. S.; Ellis, P. J.; Lay, P. A. *J. Am. Chem. Soc.* **1998**, *120*, 10827.

10.1021/ja047572u CCC: $30.25

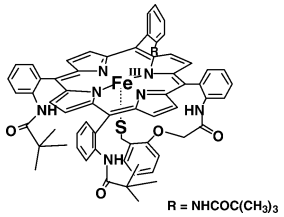

Figure 1. Synthetic heme−thiolate complex, SR complex.

unstable under the employed experimental conditions. Most of the synthesized thiolate-ligated iron porphyrins in the absence of bulky protecting groups around the axial sulfur atom were found to be very sensitive to light and air.[11−13]

Higuchi and co-workers first prepared a stable Fe^{III}−porphyrin alkanethiolate complex (SR, Figure 1), in which the thiolate ligand is sterically protected by bulky pivaloyl groups.[14] The SR(Fe^{III}) complex is known to have similar reactivity to that of cytochrome P450. Furthermore, due to the introduction of bulky groups on the RS^- coordination face of the porphyrin molecule, the thiolate complex is unique in that it retains its axial thiolate to be stable during catalytic oxidations.[15] It was also established that the thiolate ligand plays an important role in the characteristic oxidizing ability of the SR(Fe^{III}) complex, which has a marked influence on the reactivity of the high-valent iron−oxo porphyrin intermediate.[15,16]

Recently, the first synthetic SR(Fe^{III})−NO complex was prepared and characterized with the application of spectroscopic (UV−vis, EPR, and IR) and electrochemical (cyclic voltammetry) methods.[17] The studies revealed that NO coordinates reversibly to the Fe^{III} center of SR in benzene solution, and the thiolate ligand does not undergo modification during this process (e.g., formation of a nitrosothiol). The resulting SR−NO complex exhibits ν(N−O) and ν(Fe−N) modes very close to those of natural heme−thiolate-containing enzymes and differs from those of heme−imidazole-containing enzymes. The nitric oxide complex of SR(Fe^{III}) appeared to be diamagnetic (EPR-silent), whereas the parent SR complex showed a typical low-spin signal of an Fe^{III}−porphyrin−thiolate complex.[10]

Since the SR(Fe^{III}) complex reversibly binds nitric oxide, the NO−heme−thiolate adduct can be considered as a useful and valuable model for nitric oxide synthase (NOS) and nitric oxide reductase ($P450_{nor}$). Cytochrome $P450_{nor}$ is a heme enzyme that catalyzes the reduction of NO to N_2O, with electrons directly transferred from NADH ($2NO + NADH + H^+ \rightarrow N_2O + H_2O + NAD^+$).[18,19] On the basis of spectroscopic and kinetic data, Shiro et al.[20a,b] proposed that the overall enzymatic reaction involving $P450_{nor}$ consists of three chemical reactions, according to Scheme 1.

Scheme 1

$$Fe^{3+} + NO \longrightarrow Fe^{3+}NO$$
$$Fe^{3+} + NO + NADH \longrightarrow I + NAD^+$$
$$I + NO + H^+ \longrightarrow Fe^{3+} + N_2O + H_2O$$

The first intermediate of this catalytic cycle is the stable ferric−NO complex, $P450_{nor}(Fe^{III}−NO)$. Reduction of the latter by NADH yields an intermediate $[Fe−NO]^8$ complex (*I*) with an absorption maximum at 444 nm, whose identity is still controversial.[20] The formation of *I* is the rate-determining step of the overall reaction. The reactions of the wild-type and mutant forms of the $P450_{nor}$ enzyme with NO and NADH have been the subject of many spectroscopic (EPR, UV−vis, resonance Raman, infrared, and X-ray absorption),[21,22] kinetic (stopped-flow rapid scan and flash photolysis),[23] and computational (DFT and semiempirical)[24] studies. The crystal structure of the $P450_{nor}(Fe^{III}−NO)$ showed a slightly tilted and bent NO binding to the Fe^{III} atom, in contrast to the highly bent coordination found for the nitrosyl complexes of ferrous hemoproteins.[20a,21] Such a NO coordination geometry can be explained in terms of electronic (trans effect from the Cys thiolate ligand) and steric effects around the $Fe^{III}−NO$ moiety.[20]

Since the $P450_{nor}(Fe^{III}−NO)$ complex represents one of the key states in terms of understanding the molecular mechanism of catalytic reduction of NO by $P450_{nor}$, the mechanistic evaluation of the nitric oxide binding to the iron(III) porphyrin−thiolate complex has received considerable attention. Recently, we followed the reaction of nitric oxide binding to cytochrome $P450_{cam}$ kinetically and proposed detailed mechanisms and volume profiles for the NO binding to the free and camphor-bound forms of this enzyme.[25] The second-order rate constants for NO binding to $P450_{cam}$ were found to be 1.7×10^5 and 3×10^6 M^{-1} s^{-1} at 20 °C, in the absence and presence of camphor, respectively. These values appear to be much lower than that found for NO binding to $P450_{nor}$ (viz. 1.9×10^7 M^{-1} s^{-1} at 20 °C).[23] Since $P450_{cam}$ and $P450_{nor}$ are known to be similar in their structure and properties,[26] relevant questions to address include the following. Is the mechanism of NO coordination to the ferric iron of these two enzymes responsible for the difference in the biological functions between $P450_{cam}$ and $P450_{nor}$ (viz. $P450_{cam}$ does not exhibit nitric oxide reductase activity)? To what extent is NO binding controlled by the

(11) Tang, S. C.; Koch, S.; Papaefthymiou, G. C.; Foner, S.; Frankel, R. B.; Ibers, J. A.; Holm, R. H. *J. Am. Chem. Soc*. **1976**, *98*, 2414.
(12) Caron, C.; Mitschler, A.; Riviere, G.; Ricard, L.; Schapacher, M.; Weiss, R. *J. Am. Chem. Soc*. **1979**, *101*, 7401.
(13) Ogoshi, H.; Sugimoto, H.; Yoshida, Z. *Tetrahedron Lett*. **1975**, *27*, 2289.
(14) Higuchi, T.; Uzu, S.; Hirobe, M. *J. Am. Chem. Soc*. **1990**, *112*, 7051.
(15) (a) Higuchi, T.; Shimada, K.; Maruyama, N.; Hirobe, M. *J. Am. Chem. Soc*. **1993**, *115*, 7551. (b) Urano, Y.; Higuchi, T.; Hirobe, M.; Nagano, T. *J. Am. Chem. Soc*. **1997**, *119*, 12008.
(16) Higuchi, T.; Hirobe, M. *J. Mol. Catal. A: Chem*. **1996**, *113*, 403.
(17) Suzuki, N.; Higuchi, T.; Urano, Y.; Kikuchi, K.; Uchida, T.; Mukai, M.; Kitagawa, T.; Nagano, T. *J. Am. Chem. Soc*. **2000**, *122*, 12059.
(18) (a) Shoun, H.; Sudo, Y.; Beppu, T. *J. Biochem. (Tokyo)* **1983**, *94*, 1219. (b) Shoun, H.; Suyama, W.; Yasui, T. *FEBS Lett*. **1989**, *244*, 11. (c) Shoun, H.; Tanimoto, T. *J. Biol. Chem.* **1991**, *266*, 11078.
(19) Nakahara, K.; Tanimoto, K.; Hatano, K.; Usuda, K.; Shoun, H. *J. Biol. Chem.* **1993**, *268*, 8350.
(20) (a) Shimizu, H.; Obayashi, E.; Gomi, Y.; Arakawa, H.; Park, S.-Y.; Nakamura, H.; Adachi, S.; Shoun, H.; Shiro, Y. *J. Biol. Chem*. **2000**, *275*, 4816. (b) Obayashi, E.; Takahashi, S.; Shiro, Y. *J. Am. Chem. Soc*. **1998**, *120*, 12964. (c) Harris, D. L. *Int. J. Quantum Chem*. **2002**, *88*, 133. (d) Daiber, A.; Nauser, T.; Takaya, N.; Kudo, T.; Weber, P.; Hultschig, C.; Shoun, H.; Ullrich, V. *J. Inorg. Biochem*. **2002**, *88*, 343. (e) Silaghi-Dumitrescu, R. *Eur. J. Inorg. Chem*. **2003**, 1048.
(21) (a) Obayashi, E.; Tsukamoto, K.; Adachi, S.; Takahashi, S.; Nomura, M.; Iizuka, T.; Shoun, H.; Shiro, Y. *J. Am. Chem. Soc*. **1997**, *119*, 7807. (b) Shiro, Y.; Fujii, M.; Isogai, Y.; Adachi, S.; Iizuka, T.; Obayashi, E.; Makino, R.; Nakahara, K.; Shoun, H. *Biochemistry* **1995**, *34*, 9052.
(22) (a) Singh, U. P.; Obayashi, E.; Takahashi, S.; Iizuka, T.; Shoun, H.; Shiro, Y. *Biochim. Biophys. Acta* **1998**, *1384*, 103. (b) Obayashi, E.; Shimizu, H.; Park, S.-Y.; Shoun, H.; Shiro, Y. *J. Inorg. Biochem*. **2000**, *82*, 103. (c) Shimizu, H.; Park, S.-Y.; Lee, D.-S.; Shoun, H.; Shiro, Y. *J. Inorg. Biochem*. **2000**, *81*, 191. (d) Daiber, A.; Nauser, T.; Takaya, N.; Kudo, T.; Weber, P.; Hultschig, C.; Shoun, H.; Ullrich, V. *J. Inorg. Biochem*. **2002**, *88*, 343.
(23) (a) Shiro, Y.; Fujii, M.; Iizuka, T.; Adachi, S.; Tsukamoto, K.; Nakahara, K.; Shoun, H. *J. Biol. Chem*. **1995**, *270*, 1617. (b) Shiro, Y.; Kato, M.; Iizuka, T.; Nakahara, K.; Shoun, H. *Biochemistry* **1994**, *33*, 8673.
(24) Scherlis, D. A.; Cymeryng, C. B.; Estrin, D. A. *Inorg. Chem*. **2000**, *39*, 2352.
(25) Franke, A.; Stochel, G.; Jung, C.; van Eldik, R. *J. Am. Chem. Soc.* **2004**, *126*, 4181.
(26) Kizawa, H.; Tomura, D.; Oda, M.; Fukamizu, A.; Hosino, T.; Gotoh, O.; Yasui, T.; Shoun, H. *J. Biol. Chem*. **1991**, *266*, 10632.

metal−ligand system, and to what extent can the protein architecture of the active site of P450 influence the properties of the prosthetic group? What is the relative effect of an axial thiolate ligand on the ligand substitution behavior in comparison to the imidazole-ligated enzymes?

With such questions in mind, our interest has focused on a mechanistic study of the NO binding to the synthetic heme−thiolate complex (SR), which is relevant to P450 cytochrome enzymes but does not possess a protein coat. In the present study, we found that the interaction of the SR complex with excess NO in methanol solution cannot be described as a simple reversible binding of NO to the iron(III)−heme center as it was observed earlier for the cyt $P450_{cam}$/NO system. Even for a low excess of NO, a rather complex reactivity pattern involving several reaction steps was observed. The employed kinetic techniques (stopped-flow at ambient and high pressure, low-temperature stopped-flow and laser flash photolysis techniques at ambient and high pressure) allowed extraction of the appropriate rate and activation parameters for the first two reaction steps and enabled us to comment on the details of the underlying reaction mechanisms. Spectroscopic investigations of the subsequent reactions of the SR complex showed evidence for the occurrence of dynamic equilibria involving higher nitrogen oxides (NO_x) and reactive SR species. These observations are not unusual and are consistent with multiple reports in the literature describing interactions of ferric porphyrin complexes or heme proteins with a mixture of NO/NO_x species. EPR and FTIR characterization of the reaction intermediates and final product confirmed the proposed reaction pathways. The results are discussed in reference to those obtained earlier in our laboratories for the reaction of NO with imidazole-[27] and thiolate[25]-ligated iron(III) hemoproteins.

Experimental Section

Materials. All solutions were prepared in methanol or toluene from Fluka Chemika (puriss.; absolute; over molecular sieves, $H_2O \leq 0.01\%$). The iron(III) porphyrin−thiolate complex (SR) was prepared as described before in the literature[14] and characterized by FAB-MS, IR, electronic absorption spectrum, EXAFS, and elemental analysis. KNO_2 was purchased from Sigma. All other chemicals used throughout this study were of analytical reagent grade.

NO gas, purchased from Riessner Gase or Linde 93 in a purity of at least 99.5 vol %, was cleaned from trace amounts of higher nitrogen oxides, such as N_2O_3 and NO_2, by passing it through an Ascarite II column (NaOH on silica gel, Sigma-Aldrich) and then bubbling through a gas scrubbing bottle containing 5 M NaOH (Aldrich). ^{15}NO gas used for the EPR and FTIR measurements was generated by the reaction of $Na^{15}NO_2$ (ISOTEC Inc.) with diluted sulfuric acid (WAKO Pure Chemical Industries Inc.).

Solution Preparation. All solutions were prepared under strict exclusion of air oxygen. Methanol or toluene were deaerated for extended periods with pure N_2 or Ar before they were brought in contact with the SR complex or nitric oxide. The concentration of nitric oxide in NO-saturated methanol was determined to be 0.014 M at 23 °C. In toluene solution, the concentration of NO at saturation was assumed to be 0.011 M at 25 °C.[28a] Dilutions of known concentration were prepared from these saturated solutions by the use of a syringe technique.

Measurements. The concentration of free nitric oxide in methanol was determined with an ISO−NOP electrode connected to ISO−NO Mark II nitric oxide sensor from World Precision Instruments.[28b] To determine the concentration of NO in methanol solutions, the following procedure was followed. A known volume of the NO-saturated methanol solution (at 23 °C) was dropped into a known volume of degassed water. The concentration of nitric oxide in the resulting solution was measured with the NO electrode. The NO electrode was calibrated daily with fresh solutions of sodium nitrite and potassium iodide according to the method suggested by the manufacturers. The calibration factor nA/μM was determined with a linear fit program. UV−vis spectra were recorded in gastight cuvettes on a Shimadzu UV-2100 spectrophotometer equipped with a thermostated cell compartment CPS-260.

EPR Measurements. A 1 cm^3 toluene (WAKO Pure Chemical Industries Inc.) solution of SR complex (1×10^{-3} M) in a septum-capped EPR sample tube was deaerated by bubbling with argon. Then, NO (^{14}NO or ^{15}NO) gas (4 equiv to SR complex) was injected with a gastight syringe into the solution. After mixing, the sample tube was refrigerated with liquid nitrogen to 77 K, and EPR measurements were carried out. The EPR spectra were recorded with a JEOL JES-RE spectrometer.

FTIR Measurements. FTIR measurements on the SR complex in the presence of a small or a large excess of NO (^{14}NO or ^{15}NO) were performed in toluene or chloroform solutions (WAKO Pure Chemical Industries Inc.) under exclusion of air oxygen. The spectra were recorded with a JASCO FT/IR-680plus spectrophotometer.

Kinetic Measurements: Laser Flash Photolysis. Laser flash photolysis kinetic studies were carried out with the use of the LKS.60 spectrometer from Applied Photophysics for detection and an Nd:YAG laser (SURLITE I − 10 Continuum) pump source operating in the third (355 nm) harmonic (100 mJ pulses with ~7 ns pulse widths). Spectral changes at appropriate wavelength were monitored using a 100 W xenon arc lamp, monochromator, and photomultiplier tube PMT−1P22. The absorbance reading was balanced to zero before the flash, and data were recorded on a digital storage oscilloscope, DSO HP 54522A, and then transferred to a PC for subsequent analysis. Gastight quartz cuvettes and a pill-box cell combined with high-pressure equipment[29a] were used at ambient and under high pressure (up to 160 MPa), respectively. At least 20 kinetic runs were recorded under all conditions, and the reported rate constants represent the mean value of these. For time-resolved optical (TRO) absorption measurements, a photomultiplier tube (PMT) detector was employed to obtain kinetic traces at a single observation wavelength. TRO spectra were recorded point by point using a monochromator in the optical train to vary the observation wavelength.

Stopped-Flow Kinetics. Stopped-flow studies on the reaction of NO with the SR complex were carried out using an SX-18MV (Applied Photophysics) stopped-flow spectrometer. Deoxygenated methanol solutions of SR were rapidly mixed with solutions of various [NO], and the changes in absorbance at appropriate wavelengths were monitored.

High-Pressure Stopped-Flow. High-pressure stopped-flow experiments were performed on a custom-built instrument described previously[29b,c] at pressures up to 130 MPa. Kinetic traces were recorded on an IBM-compatible computer and analyzed with the OLIS KINFIT (Bogart, GA, 1989) set of programs.

Low-Temperature Stopped-Flow Instrument and Software. Time-resolved UV−vis spectra were recorded with a Hi-Tech SF-3L low-temperature stopped-flow unit (Hi-Tech Scientific, Salisbury, U.K.) equipped with a J&M TIDAS 16/300−1100 diode array spectrophotometer (J&M, Aalen, Germany). The optical cell had a light path of 1.0 cm and was connected to the spectrophotometer unit with flexible

(27) Lavermann, L. E.; Wanat, A.; Oszajca, J.; Stochel, G.; Ford, P. C.; van Eldik, R. *J. Am. Chem. Soc.* **2001**, *123*, 285.
(28) (a) Shaw, A. W.; Vosper, A. J. *J. Chem. Soc., Faraday Trans. 1* **1977**, *73* (8), 1239. (b) Kudo, S.; Bourassa, J. S. E.; Sato, Y.; Ford, P. C. *Anal. Biochem.* **1997**, *247*, 193.
(29) (a) Spitzer, M.; Gartig, F.; van Eldik, R. *Rev. Sci. Instrum.* **1988**, *59*, 2092. (b) van Eldik, R.; Palmer, D. A.; Schmidt, R.; Kelm, H. *Inorg. Chim. Acta* **1981**, *50*, 131. (c) van Eldik, R.; Gaede, W.; Wieland, S.; Kraft, J.; Spitzer, M.; Palmer, D. A. *Rev. Sci. Instrum.* **1993**, *64*, 1355.

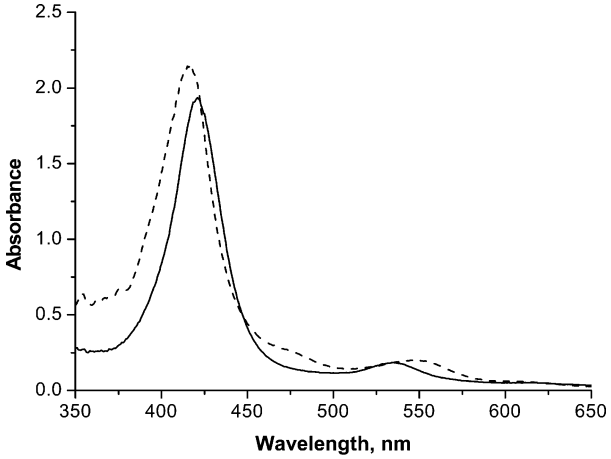

Figure 2. Electronic absorption spectra of the SR complex and NO in methanol solution as separate solutions (solid line) and after NO saturation (dashed line). Experimental conditions: [SR] = 1.3×10^{-5} M, [NO] = 1.41×10^{-2} M in methanol, $T = 25$ °C.

light guides; 5 mL driving syringes were used. The mixing chamber was immersed in an ethanol bath which was placed in a dewar flask containing liquid nitrogen. The ethanol bath was cooled by liquid nitrogen evaporation, and its temperature was measured by using a Pt resistance thermometer and maintained to ±0.1 °C by using a PID temperature-controlled thyristor heating unit (both Hi-Tech). Complete spectra were collected between 340 and 1100 nm with the integrated J&M software, Kinspec 2.30.

All kinetic experiments were performed under pseudo-first-order conditions, that is, at least a 10-fold excess of NO. The studied reactions exhibited pseudo-first-order behavior for at least three half-lives. In all stopped-flow experiments, at least five kinetic runs were recorded under all conditions, and the reported rate constants represent the mean values.

Results

The UV−vis spectrum of the SR complex in methanol solution exhibits a Soret band maximum at 421 nm and a Q-band at 534 nm (Figure 2). Exposure of the degassed solutions of SR to an excess of NO leads to spectral shifts of the Soret and Q-bands to 416 and 546 nm, respectively. The uptake of NO appears to be irreversible as judged from experiments in which a stream of Ar gas was used to remove NO from the solution. This can indicate that either the equilibrium of the nitrosylation reaction (eq 1) is strongly shifted to the nitrosyl product or

$$\mathrm{SR} + \mathrm{NO} \underset{k_{\mathrm{off}}}{\overset{k_{\mathrm{on}}}{\rightleftharpoons}} \mathrm{SR(NO)} \quad K_{\mathrm{NO}} \tag{1}$$

subsequent reactions occur in the presence of a large excess of NO that produce a very stable nitrosyl complex. Spectral changes recorded for this reaction in methanol solution with the diode array detector of the low-temperature stopped-flow spectrophotometer indicated that even for a low excess of NO, the interaction between the SR complex and NO is much more complex than shown in eq 1 and involves subsequent reaction steps. These observations are confirmed by the results obtained from EPR and FTIR measurements on the SR complex solution after addition of an equivalent[17] or an excess of nitric oxide (this study).

I. Stopped-Flow Kinetics of the SR(NO) Complex Formation Reaction. Figure 3 reports typical spectral changes

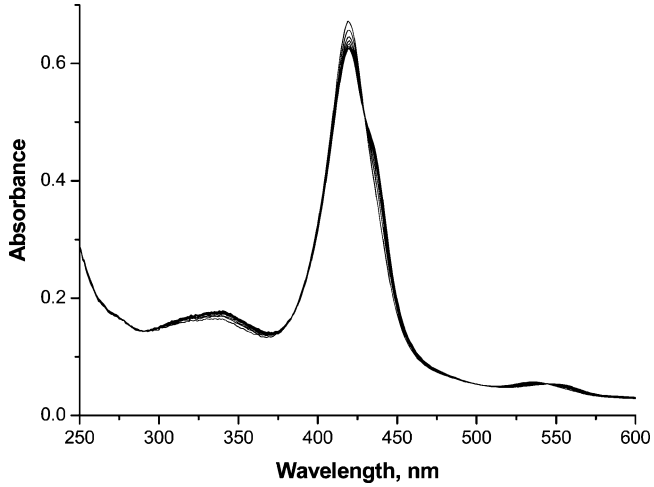

Figure 3. Typical spectral changes measured immediately after stopped-flow rapid mixing of a methanol solution of SR with a 20-fold excess of NO at 5 °C. Experimental conditions: [SR] = 4.3×10^{-6} M, [NO] = 9×10^{-5} M in methanol solution; spectra recorded within the time of 0−0.05 s after mixing.

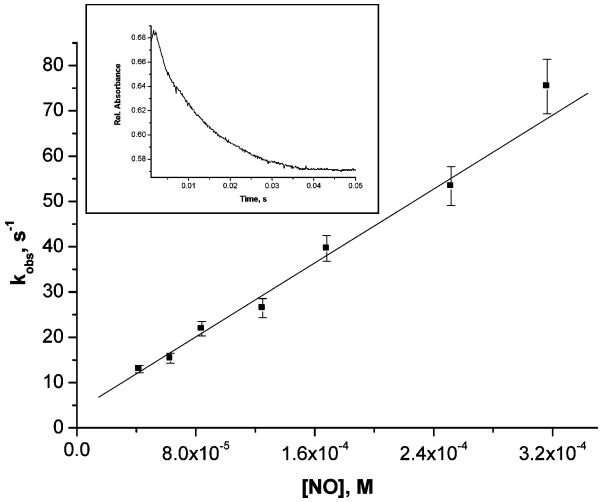

Figure 4. NO concentration dependence of k_{obs} for the formation of SR(NO). Experimental conditions: [SR] = 4.7×10^{-6} M in methanol solution at 5 °C, $\lambda_{\mathrm{det}} = 420$ nm. Inset: typical absorbance−time plot recorded for the SR(NO) complex formation at [SR] = 4.7×10^{-6} M, [NO] = 1.9×10^{-4} M, $T = 5$ °C, $\lambda_{\mathrm{det}} = 420$ nm.

monitored at 5 °C immediately after stopped-flow rapid mixing of a methanol solution of SR with a small (20-fold) excess of NO.

Spectra are characterized by the appearance of a new band at 435 nm and a shift in the Q-band from 534 to 552 nm with clean isosbestic points at 428.5, 508.5, and 545 nm. Absorbance−time traces recorded at 420 nm show that the studied reaction is very fast and occurs within 50 ms at 5 °C and [NO] = 1.9×10^{-4} M (inset in Figure 4). It is suggested that this process represents rapid SR(NO) complex formation, as indicated in reaction 1. The rate of reaction 1 with NO in excess (10−80-fold) proved to follow pseudo-first-order kinetics for which the observed rate constant, k_{obs}, is expressed by eq 2.

$$k_{\mathrm{obs}} = k_{\mathrm{on}}[\mathrm{NO}] + k_{\mathrm{off}} \tag{2}$$

According to eq 2, a plot of k_{obs} versus [NO] was found to be linear (Figure 4) with a slope $k_{\mathrm{on}}^{(1)} = (2.2 \pm 0.1) \times 10^5$ M^{-1} s^{-1} and an intercept $k_{\mathrm{off}}^{(1)} = 1.8 \pm 2.1$ s^{-1} at 5 °C. The value

Table 1. Rate Constants and Activation Parameters for the First and Second Reaction Steps of NO with the SR Complex Determined by Stopped-Flow

		first reaction	second reaction	
T (°C)	pressure (MPa)	$k_{on} \times 10^{-5}$ ($M^{-1} s^{-1}$)	$k_{on} \times 10^{-4}$ ($M^{-1} s^{-1}$)	$k_{on} \times 10^{-3}$ ($M^{-1} s^{-1}$)
−55	0.1			1.6 ± 0.2
−50				2.1 ± 0.2
−45				2.6 ± 0.3
−40				3.8 ± 0.4
−30				6.2 ± 0.5
5		2.2 ± 0.1	2.71 ± 0.05	
10		5.3 ± 0.3	3.18 ± 0.02	
15		8.3 ± 0.2	3.62 ± 0.02	
20		14 ± 1	4.30 ± 0.04	
25		27 ± 2	4.83 ± 0.04	
30		44 ± 2		
−2	10		3.77 ± 0.06	
	50		5.11 ± 0.12	
	90		7.14 ± 0.16	
	130		8.98 ± 0.10	
5	10	1.2 ± 0.3		
	50	1.1 ± 0.2		
	90	1.0 ± 0.3		
	130	0.8 ± 0.1		
$\Delta H^{\ddagger}$ (kJ mol^{-1})		75 ± 3	17.6 ± 0.6	22.6 ± 0.9
$\Delta S^{\ddagger}$ (J $mol^{-1} K^{-1}$)		+130 ± 11	−96 ± 2	−78 ± 4
$\Delta V^{\ddagger}$($cm^3 mol^{-1}$)		+6.4 ± 1.0	−16.3 ± 0.8	

of k_{off} is too small to be determined accurately by extrapolation of the stopped-flow data; however, it may be possible to measure it in a more direct way, for example, by using an NO-trapping technique.[30,31] However, the studied system seems not to be suitable for such NO-trapping measurements due to the subsequent reactions that follow formation of the SR(NO) complex. It was, therefore, not possible to measure k_{off} in a direct way.

Since NO binds very rapidly to the SR complex, the temperature and pressure dependence of the "on" reaction could be studied using stopped-flow techniques for low NO concentration conditions. For that reason, the reaction of NO with the SR complex was studied at [NO] = 7×10^{-5} M over the temperature range of 5−30 °C, and the k_{on} values are summarized in Table 1. The Eyring plot constructed on the basis of these data was found to be linear (Figure S1 in Supporting Information) and gave $\Delta H_{on}^{\ddagger(1)} = 75 \pm 3$ kJ mol^{-1} and $\Delta S_{on}^{\ddagger(1)} = +130 \pm 11$ J $mol^{-1} K^{-1}$. The value of the activation volume obtained from the pressure dependence of k_{obs} (inset in Figure S1, Table 1) was found to be positive, $\Delta V_{on}^{\ddagger(1)} = +6.4 \pm 1.0$ cm^3 mol^{-1}.

II. Spectroscopic and Kinetic Studies on the Subsequent Reactions. On a longer time scale (inset in Figure 5), under conditions of 40-fold excess of NO at 5 °C, the band at 435 nm representing the SR(NO) complex disappears with the concomitant appearance of a new band at 419.5 nm (Figure 5).

The spectrum of the resulting species resembles the absorption spectrum of the parent SR complex in methanol solution, but its Soret band intensity appears to be much higher than that of the SR complex. Moreover, there is a significant difference in the Q-band region of these two spectra (Q-band maximum at 534 and 542 nm for the SR complex and a new species, respectively). EPR and FTIR measurements of the SR toluene

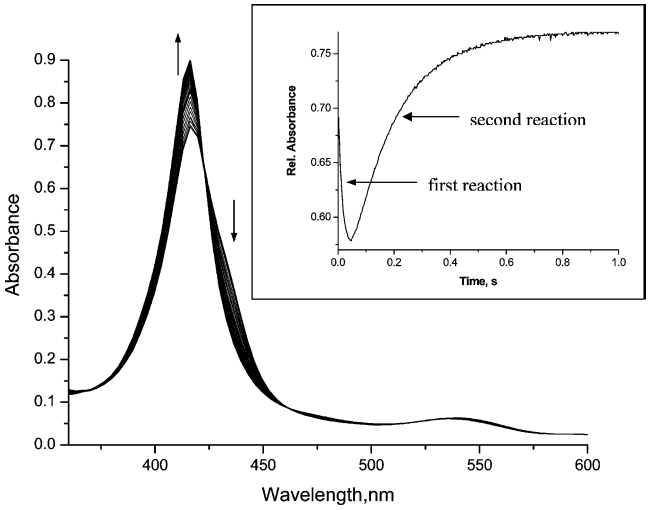

Figure 5. Representative spectral changes and typical absorbance−time plots at 420 nm (inset) for the reaction of the SR complex with NO measured with the stopped-flow instrument at [SR] = 4.7×10^{-6} M, [NO] = 1.9×10^{-4} M, T = 5 °C; spectra recorded within the time of 0−1 s after mixing.

solution under conditions of a small excess of NO (only 4 equiv to SR) confirmed the formation of a new species. Its EPR spectrum (Figure 6b,c) resembles spectra characteristic for five-coordinate NO−heme (Fe^{II}) complexes.[32a] The IR spectrum of the new complex (Figure 7a) shows a sharp band at 1604 cm^{-1}, which seems to be very similar to the N−O stretching modes found for nitrosylhemoglobin and other NO═Fe(II) porphyrins.[32b]

The rate of the second reaction was shown to depend on the NO concentration. The plot of k_{obs} versus [NO] (ranging from 7.1×10^{-4} to 5.0×10^{-3} M) was found to be linear with an almost zero intercept within the experimental error limits ($k_{off}^{(2)} = 0.6 \pm 3.6$ s^{-1}, inset in Figure 8). The resulting second-order rate constant, $k_{on}^{(2)}$, determined from the slope of this plot equals $(2.71 \pm 0.05) \times 10^4$ $M^{-1} s^{-1}$ at 5 °C. The rate constants measured at [NO] = 7.08×10^{-4} M over the temperature range of 5−25 °C are summarized in Table 1. The corresponding Eyring plot was found to be linear and resulted in $\Delta H_{on}^{\ddagger(2)} = 17.6 \pm 0.6$ kJ mol^{-1} and $\Delta S_{on}^{\ddagger(2)} = -96 \pm 2$ J mol^{-1} K^{-1}.

The use of a low-temperature stopped-flow instrument enabled us to measure the temperature dependence of the reaction as a function of [NO] in a more extended NO concentration range (from 7.1×10^{-4} to 7.0×10^{-3} M) over the temperature range of −55 to −30 °C. Plots of k_{obs} versus [NO] were linear at all temperatures, and the resulting k_{on} values are summarized in Table 1. The corresponding Eyring plot was found to be linear and resulted in $\Delta H_{on}^{\ddagger(2)} = 22.6 \pm 0.9$ kJ mol^{-1} and $\Delta S_{on}^{\ddagger(2)} = -78 \pm 4$ J mol^{-1} K^{-1}, which are in reasonable agreement with the values measured at higher temperatures (see Table 1, Figure 8). The effect of pressure on the kinetics of the NO binding reaction was examined over the pressure range of 0.1−130 MPa at −2 °C (data are summarized in Table 1), and the plot of ln(k_{obs}) versus pressure was linear, with $\Delta V_{on}^{\ddagger} = -16.3 \pm 0.8$ cm^3 mol^{-1}.

For a 40-fold excess of NO at 5 °C, the first two fast reactions discussed above are followed by much slower subsequent processes. Spectral evaluation of the reaction followed up to

(30) Schneppensieper, T.; Wanat, A.; Stochel, G.; Goldstein, S.; Meyerstein, D.; van Eldik, R. *Eur. J. Inorg. Chem.* **2001**, 2317.
(31) Wanat, A.; Schneppensieper, T.; Karocki, A.; Stochel, G.; van Eldik, R. *J. Chem. Soc., Dalton Trans.* **2002**, 941.
(32) (a) O'Keeffe, D. H.; Ebel, R. E.; Peterson, J. A. *J. Biol. Chem.* **1978**, *253* (10), 3509. (b) Scheidt, W. R.; Duval, H. F.; Neal, T. J.; Ellison, M. K. *J. Am. Chem.* Soc. **2000**, *122*, 4651.

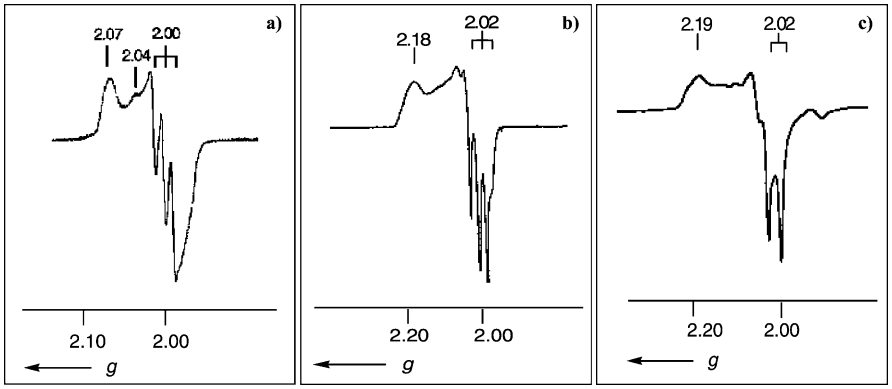

Figure 6. EPR spectra of 1 mM SR complex in toluene at 77 K after addition of (a) 1 equiv of ^{14}NO gas and subsequent reduction with $NABH_4$/18-crown-6 (adapted from ref 17); (b) 4 equiv of ^{14}NO; and (c) 4 equiv of ^{15}NO.

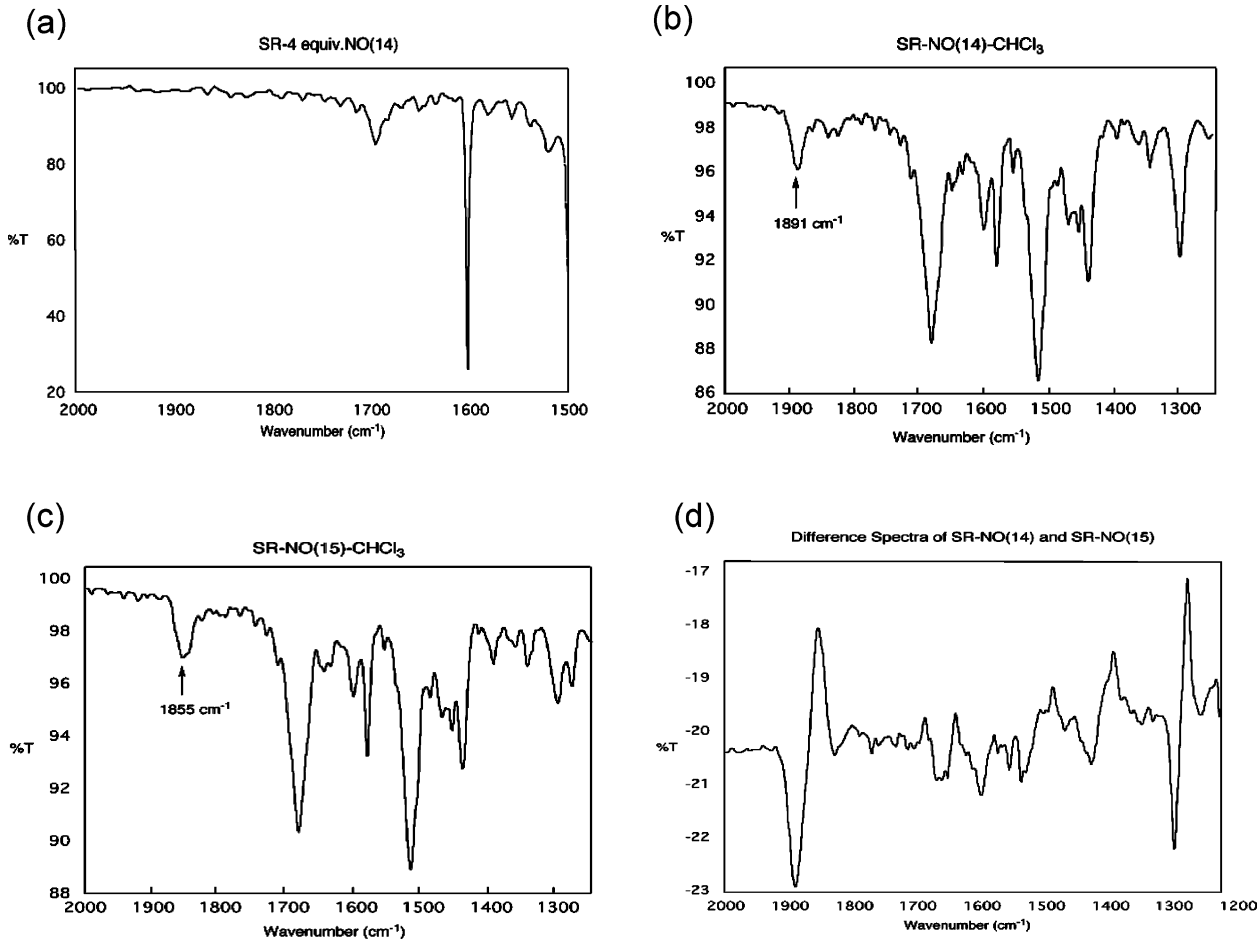

Figure 7. Figure 7. FTIR spectra of (a) the toluene solution of the SR complex with 4 equiv of ^{14}NO; (b) the chloroform solution of the SR complex under conditions of a large excess of ^{14}NO; (c) the chloroform solution of the SR complex under conditions of a large excess of ^{15}NO; and (d) the difference spectrum between (b) and (c).

1000 s with the diode array detector of the stopped-flow spectrophotometer (Figure S2a in Supporting Information) indicates a slow absorbance increase at 419.5 nm within ca. 300 s, followed by an even slower decrease in absorbance with a concomitant slight shift in the Soret band to shorter wavelengths (~416 nm) and the appearance of a very weak shoulder at 430 nm (isosbestic point at 414 nm). Observations made using single wavelength detection at 420 nm were consistent with the diode array studies. As can be seen from Figure S2a, the reaction characterized by the slow absorbance decrease is still not complete under the selected conditions (40-fold excess of NO, 5 °C, t = 1000 s). It should further be noted that absorbance changes related to the last two processes were found to be *much smaller* (10−15 times) than those observed for the first two fast reaction steps.

When the reaction was studied under conditions of a large NO excess at 10 °C, the first three reactions appeared to be too fast for the stopped-flow time scale and only the slowest process described by the absorbance decrease can be clearly observed under such conditions. As shown in Figure S2b, it occurs within 0.5 s at [NO] = 7.1×10^{-3} M and is accompanied by a slight blue shift of the Soret band and the appearance of a new

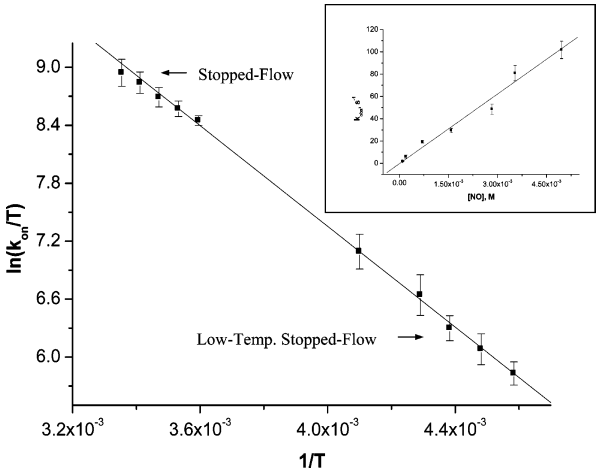

Figure 8. Eyring plot of $\ln(k_{on}/T)$ versus $1/T$ for the second reaction of the SR complex with nitric oxide as measured with the stopped-flow and low-temperature stopped-flow technique. Experimental conditions: [SR] = 2×10^{-6} M, [NO] = 7.1×10^{-4} M in methanol, $\lambda_{det} = 416$ nm. Inset: Plot of k_{obs} versus [NO] for the second reaction of the SR complex with NO. Experimental conditions: [SR] = 2×10^{-6} M in methanol, $T =$ 5 °C, $\lambda_{det} = 416$ nm.

shoulder at 432 nm, with isosbestic points at 414 and 428 nm. Notably, in this case, the intensity of the shoulder at 430 nm is much higher than that observed under conditions of lower NO concentrations. At longer times (Figure S2c), the absorbance decrease is followed by a significant intensity increase at 416 nm (with isosbestic points at 425 and 447 nm), which finally leads to the end spectrum observed after exposure of the degassed solutions of SR to an excess of NO (see Figure 2). There were no further spectral changes observed under such conditions.

The FTIR spectrum recorded for a chloroform solution of the SR complex under conditions of a large excess of nitric oxide (Figure 7b) differs completely from that obtained after addition of only 4 equiv of NO (compare Figure 7a). It is characterized by new bands at 1891 and 1301 cm^{-1} with ^{15}N isotope shifts of about 36 and 20 cm^{-1}, respectively (Figure 7c,d).

III. Spectroscopic Studies on the SR/NO System in the Presence of Higher Nitrogen Oxides (NO_x). Since it is practically impossible to prepare NO solutions totally free of higher nitrogen oxides,[33] it is possible that NO_x impurities can interfere with the studied reaction and account for the observed behavior (such as the subsequent reaction steps). For that reason, the reaction between the SR complex and nitrite, as well as the reaction between the SR complex and NO in the presence of higher nitrogen oxides (N_2O_3 and NO_2^-), was studied in more detail.

A. Reaction of the SR Complex with NO_2^-. Treating the SR complex with 3 mM KNO_2 solution at 10 °C led to rather complex spectral changes: a rapid absorbance increase at 421 nm complete within 22 s (Figure S3a in Supporting Information), followed by a slower decrease with an isosbestic point at 414 nm and a concomitant slight shift of the Soret band to 419 nm, and finally followed by a slow absorbance increase at 416 nm (Figure S3b). It should be noted that the final product of the reaction between the SR complex and nitrite seems to be spectrally indistinguishable from that obtained under conditions of a large excess of NO (Figure S2c). However, in this case, the reaction steps leading to the final product appear to be *much slower* than that observed for the reaction with a large excess of NO.

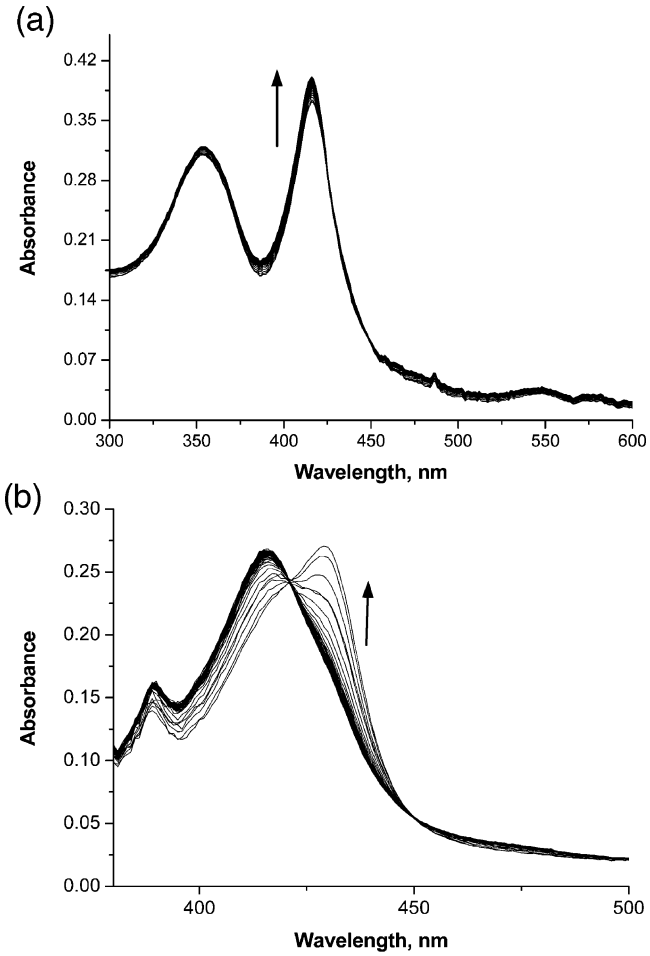

Figure 9. Representative spectral changes measured with the stopped-flow instrument after mixing methanol solutions of 4.8×10^{-6} M SR complex and 7.1×10^{-3} M of NO (a) in the presence of 3.0×10^{-3} M KNO_2^-, at 10 °C, spectra recorded within the time of 0−200 s after mixing; and (b) after introduction of small quantities of air, spectra recorded within the time of 0−1 s, at 10 °C.

B. Reaction of the SR Complex with a Large Excess of NO in the Presence of NO_2^-. Addition of 3 mM nitrite to the system containing the SR complex in the presence of a large excess of NO resulted in spectral changes that led to the same final product with a maximum band at 416 nm (Figure 9a). Noteworthy, under such conditions, the last reaction step described by the absorbance increase at 416 nm becomes much faster.

C. Reaction of the SR Complex with a Large Excess of NO in the Presence of N_2O_3. Spectral changes recorded for the solution containing the SR complex and a large excess of NO after introduction of small quantities of air appeared to be very similar to those measured for the system without addition of oxygen and led to the same final product with the Soret band at 416 nm. However, it is important to note that the presence of a small amount of oxygen *significantly* accelerated the formation of the band at 430 nm (Figure 9b), with an intensity

(33) (a) Wolak, M.; Stochel, G.; Hamza, M.; van Eldik, R. *Inorg. Chem.* **2000**, *39*, 2018. (b) Awad, H. H.; Stanbury, D. M. *Int. J. Chem. Kinet.* **1993**, *25*, 375. (c) Feelish, M. *J. Cardiovasc. Pharmacol.* **1991**, *17*, 25. (d) Ford, P. C.; Wink, D. A.; Stanbury, D. M. *FEBS Lett.* **1993**, *326*, 1.

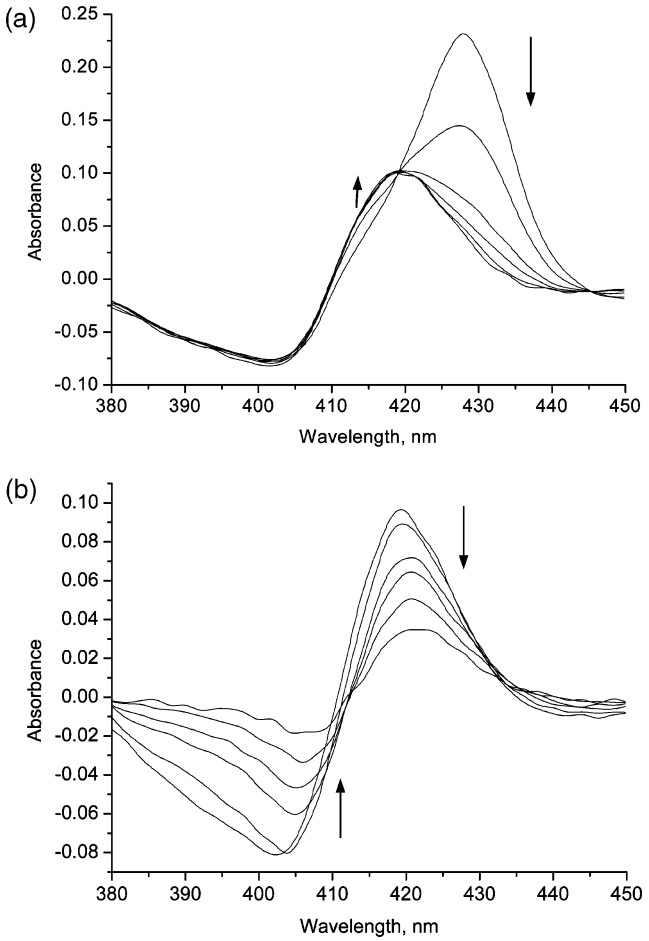

Figure 10. Transient absorption difference spectra recorded for the SR/NO system following laser flash photolysis at 355 nm. Successive measurements after delays of (a) 14.6 μs to 0.44 ms and (b) 1.5−44 ms. Experimental conditions: [SR] = 1×10^{-5} M, [NO] = 9.4×10^{-3} M in methanol, $T = 25$ °C.

much higher in comparison to that of the system in the absence of oxygen (only a weak shoulder in Figure S2a,b).

IV. Laser Flash Photolysis Studies. Laser flash photolysis can be employed to study the kinetics of reactions on a much faster time scale than stopped-flow techniques. We expected that the use of this technique could provide important information on photochemically produced intermediates formed after flash photolysis of an equilibrium mixture of SR/SR(NO) and may, therefore, offer a strategy to study the subsequent thermal reactions.

A. Laser Flash Photolysis of the SR/SR(NO) Equilibrium Mixture. All flash photolysis studies on the SR/SR(NO) system were carried out in methanol solution for different NO concentrations ([NO]/[SR] ≥ 10) using photoexcitation at 355 nm. Attempts to use 532 nm irradiation were not successful due to the very low photoreactivity at this wavelength. Figure 10 reports typical transient difference spectra recorded after flash photolysis of an equilibrium mixture of SR/SR(NO), immediately after the flash (14.6 μs) and after delays of 39.1 μs to 44 ms. The TRO spectra indicate that the observed photoreaction is not simply a displacement of the NO ligand from the studied nitrosyl complex. Immediately after the flash, transient difference spectra are characterized by a bleaching centered at 402 nm and a prompt transient absorption at 428 nm. The spectra collected after delays of 14.6−0.44 ms (Figure 10a) clearly show the disappearance of the positive peak at 428 nm with concomitant formation of a new transient absorption centered at 420 nm (isosbestic points at 420 and 444 nm). Subsequently, the transient absorption and bleaching disappear within 44 ms with a slight shift of the latter from 402 to 405 nm (Figure 10b). A typical kinetic trace recorded at a single wavelength clearly indicates multiple processes, that is, one reaction occurring on the microsecond and two on the millisecond time scale (Figure S4 in Supporting Information). The rates of the first and second photoinduced reactions were found to depend on the NO concentration, with k_{obs} being first order in [NO]. From the slopes of the plots of k_{obs} versus [NO] (Figure S5 in Supporting Information), second-order rate constants (i.e., k_1 and k_2 for the first and second reactions, respectively) were calculated. The first, short-lived intermediate, with λ_{max} at 428 nm, decayed very rapidly with $k_1 = (1.21 \pm 0.03) \times 10^8$ M^{-1} s^{-1} at 25 °C. The second transient species decayed more slowly, with $k_2 = (4.09 \pm 0.08) \times 10^4$ M^{-1} s^{-1}. The third intermediate decayed on a longer time scale and finally led to the full regeneration of the initial spectrum. However, due to *very small* absorbance changes, the third and slowest reaction could not be studied in more detail.

Table 2. Rate Constants and Activation Parameters for the Reaction of NO with the SR Complex Determined by Laser Flash Photolysis

T (°C)	pressure (MPa)	$k_2 \times 10^{-4}$ (M^{-1} s^{-1})
5	0.1	1.86 ± 0.03
10		2.27 ±0.07
15		2.69 ± 0.05
20		
25		4.09 ± 0.08
30		
35		4.9 ± 0.2
25	40	6.8 ± 0.2
	80	8.8 ± 0.3
	120	11.3 ± 0.5
	160	15.1 ± 0.7
$\Delta H^{\ddagger}$ (kJ mol^{-1})		22 ± 2
$\Delta S^{\ddagger}$ (J mol^{-1} K^{-1})		−86 ± 5
$\Delta V^{\ddagger}$ (cm^3 mol^{-1})		−16.1 ± 0.2

More detailed kinetic measurements were performed for the second process, making use of the flash photolysis technique. The effect of temperature on the second reaction was examined in the range of 5−35 °C, and the resulting k_2 values are reported in Table 2. An Eyring plot for these data was found to be linear, which resulted in $\Delta H_2^{\ddagger} = 22 \pm 2$ kJ mol^{-1} and $\Delta S_2^{\ddagger} = -86 \pm 5$ J mol^{-1} K^{-1}. As can be seen from the results reported in Table 2, the second-order rate constants for the studied reaction (k_2) increase significantly with increasing pressure. The plot of ln(k_{obs}) versus pressure gave a straight line, which resulted in a substantially negative volume of activation, $\Delta V_2^{\ddagger} = -16.1 \pm 0.2$ cm^3 mol^{-1} at 25 °C.

B. Laser Flash Photolysis Studies on the SR/NO_2^- System. We reported above for the stopped-flow experiments that in the presence of an excess of NO, rapid binding of NO to the SR complex is followed by subsequent slower reactions. This means that under the selected conditions, the solution of SR with NO subjected to flash photolysis experiments contains the product(s) of the subsequent reactions. For that reason, attention was given to the photochemical properties of the SR/NO_2^- system. As can be seen from Figure 11, the time-resolved spectra

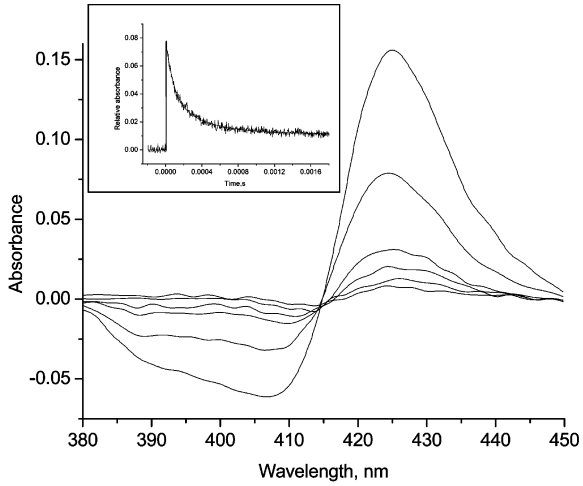

Figure 11. Transient absorption difference spectra recorded for the SR/NO_2^- system following laser flash photolysis at 355 nm. Successive measurements after delays of 58.6 μs to 1.80 ms. Inset: Typical example of flash photolysis kinetic traces recorded at $\lambda_{det} = 425$ nm for the SR complex with an excess of nitrite. Experimental conditions: [SR] = 1×10^{-5} M, [NO_2^-] = 1×10^{-2} M in methanol, $T = 25$ °C.

recorded during photolysis of the SR complex in the presence of a large excess of NO_2^- can be described by prompt transient bleaching and a transient absorption centered at 407 and 425 nm, respectively. These difference spectra resemble those observed for the first (and fastest) step of the reaction between NO and the SR complex (see Figure 10a), but the bands characteristic for the transient bleaching and transient absorption are slightly shifted to shorter (407 → 402 nm) and longer (425 → 428 nm) wavelengths, respectively. Typical absorbance versus time plots at 410 and 420 nm (inset in Figure 11) were found to be consistent with two exponential functions. A detailed kinetic examination of these reactions revealed no dependence on the nitrite concentration. On the basis of these findings and the results obtained in the stopped-flow experiments, it can be concluded that the reactions observed following flash photolysis of a solution of the SR complex containing nitrite do not represent a simple nitrite photolabilization reaction from the suggested SR(NO_2^-) complex.

C. Laser Flash Photolysis of the Parent SR Complex in Methanol Solution. The results reported above have stimulated a search for more information on the photochemical properties of the SR/NO system. In view of the fact that flash photolysis of the SR(NO) complex at 355 nm led to the formation of transient species that decayed to reproduce the starting spectrum, the possibility of a photoinduced degradation of the studied complex can be excluded. Notably, flash photolysis of the parent SR complex in the absence of NO (Figure S6 in Supporting Information) gave prompt transient bleaching with a minimum at 415 nm and a transient absorption maximum at 428 nm. Furthermore, although photoinduced absorbance changes of SR decayed back to the original spectrum within ca. 44 ms, residual absorbance changes did persist. This finding is consistent with the steady-state absorption spectra of the SR complex recorded before and immediately after flash photolysis (inset in Figure S6), where a slight absorbance decrease and shift to longer wavelengths in the Soret region was observed. In contrast, for the SR solution in the presence of an excess of NO, no significant permanent photochemistry was observed. Since all

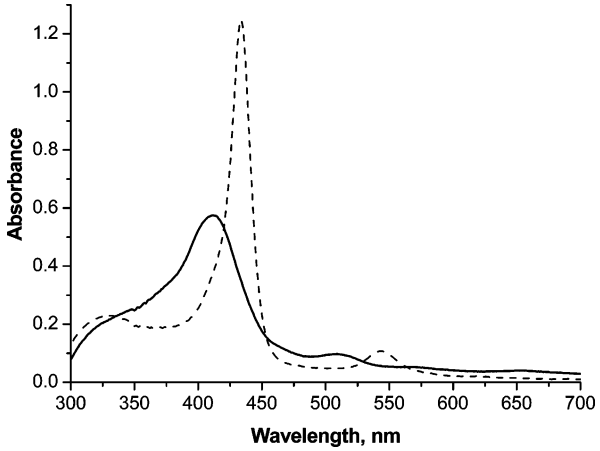

Figure 12. Electronic absorption spectra of the SR complex and NO as separate solutions (solid line) and after NO saturation (dashed line) in toluene solution. Experimental conditions: [SR] = 4×10^{-6} M, [NO] = 1.15×10^{-2} M in toluene, $T = 25$ °C.

flash photolysis experiments were carried out in an excess of NO, the observed photoinduced degradation of the parent SR complex should not affect the kinetics of the studied reaction.

V. Reactions of the SR Complex with NO in Toluene. Since methanol can be involved in the facile nucleophilic attack at coordinated nitrosyl and lead to the reductive nitrosylation of the ferric porphyrins,[34] the reaction between the SR complex and nitric oxide was carried out in toluene, a highly hydrophobic solvent. The absorption spectrum of SR measured in toluene is clearly distinguishable from that obtained in methanol solution and is characterized by the blue-shifted Soret and visible bands to 411 and 508 nm, respectively (see Figures 2 and 12). Addition of NO to the degassed SR toluene solution results in the spectral shifts of the Soret and Q-bands to 433 and 543.5 nm, respectively (Figure 12). However, as it was concluded from the absorption changes recorded for this reaction with the diode array detector of the stopped-flow spectrophotometer at low temperature, interaction of the SR complex with NO in toluene solution is much more complex and involves more reaction steps and intermediates which finally lead to the spectrum characterized by the Soret band maximum at 433 nm. Rapid stopped-flow mixing of a toluene solution of SR with an excess of NO at −50 °C resulted in a decrease in absorbance of the Soret band at 411 nm and an increase in absorbance at 439 nm. The reaction takes place within 0.4 s with $k_{obs} = 20.1 \pm 1.7$ s^{-1} at −50 °C and [NO] = 2.9×10^{-4} M (inset in Figure S7 in Supporting Information). On a longer time scale (40 s), the first fast reaction step is followed by the next slower reaction ($k_{obs} = 0.73 \pm 0.3$ s^{-1} at −50 °C), which is characterized by the absorbance decrease at 439 nm and the appearance of a new band maximum at 425 nm (Figure S7). Finally, a significant intensity decrease at 425 nm is observed, and the end spectrum with a Soret band at 433 nm is formed. This experiment shows that even in nonpolar solvents, interaction of the SR complex with an excess of NO cannot be regarded as a simple reversible binding of NO to the iron(III) center and involves subsequent reaction steps as observed in methanol solution.

(34) (a) Mu, X. H.; Kadish, K. M. *Inorg. Chem.* **1988**, *27*, 4720. (b) Gwost, D.; Caulton, K. G. *J. Chem. Soc., Chem. Commun.* **1973**, 64. (c) Gwost, D.; Caulton, K. G. *Inorg. Chem.* **1973**, *12*, 2095.

Discussion

Equilibrium and Rate Constants for SR(NO) Complex Formation. The axial coordination sites of Fe(III) in SR are occupied by a thiolate sulfur as the fifth and a methanol molecule as the sixth ligand.[14] Since the RS coordination face of the porphyrin molecule is protected by bulky groups, it is assumed that the first fast reaction observed immediately after stopped-flow mixing of a methanol solution of SR with a small excess of NO represents rapid displacement of CH_3OH by NO and leads to formation of the six-coordinate SR(NO) complex. It appears to be EPR-silent due to coupling of the two unpaired electrons from the Fe and NO orbitals.[17] Upon reduction with $NaBH_4$/18-crown-6, a characteristic EPR spectrum of the six-coordinate thiolate−Fe^{II}(porphyrin)−NO complex[32] appeared (Figure 6a).[17] The ν(N−O) mode in the SR(III)−NO complex found by IR spectroscopy (at 1826 cm^{-1} and shifted to 1792 cm^{-1} upon substitution by ^{15}NO) suggests that thiolate coordination in the SR complex still remains following the reaction of the SR with an equivalent amount of nitric oxide.[17] The overall process can be summarized as follows:

$$SR(MeOH) + NO \rightleftarrows SR(NO) + MeOH$$

The binding of NO to SR was found to be very fast with a second-order rate constant of $k_{on} = (2.7 \pm 0.2) \times 10^6\ M^{-1}\ s^{-1}$ at 25 °C. Since the synthetic NO−heme−thiolate complex is regarded as a model for cytochrome P450 enzymes, it is informative to compare the k_{on} values determined for the present system with those found for NO binding to the native forms of ferriheme−thiolate proteins. As seen from Table 3, association rate constants for NO with Fe^{III}−heme−thiolate proteins range from 3.2×10^5 (for substrate-free $P450_{cam}$ at 25 °C) to $1.9 \times 10^7\ M^{-1}\ s^{-1}$ (for nNOS at 23 °C). A comparison of these k_{on} values with that determined in the present study demonstrates that the SR complex can be considered as a reasonable model for the kinetics of the analogous reactions with Fe^{III}−heme−thiolate proteins. Furthermore, since in all of the systems reported in Table 3, NO binds to the thiolate-ligated Fe^{III}−heme, the apparent differences in the k_{on} values should indeed reflect the influence of the protein structure in the heme binding pocket (electrostatic and steric environment in the neighborhood of the iron center) on the NO binding kinetics as well the lability of the leaving group (or its absence). The $P450_{nor}$ and NOS enzymes are more reactive than the SR complex, indicating that in these cases, the protein or the lability of the sixth axial ligand should accelerate the nitrosylation processes. The reactivity of substrate-free $P450_{cam}$ toward NO is much lower than that of the model SR complex. In contrast, NO binding to camphor-bound $P450_{cam}$ appears to be much faster than that of the substrate-free form[25] and is almost comparable to that of the SR complex. Since in this case, NO binds to Fe(III) centers with different coordination spheres (viz. six- and five-coordinate Fe(III) for the substrate-free and camphor-bound $P450_{cam}$, respectively), the reaction dynamics seems to be far more dominated by the nature of the metal center than by the protein architecture.

It is reasonable to expect that changing the proximal ligand would have a significant effect on the reactivity of the Fe^{III}−heme center. Due to the anionic nature of the RS^- group, it is clear that the iron atom in the thiolate-ligated heme proteins should be stabilized in its higher (Fe^{III}) oxidation state. In general, the k_{on} values found for the model SR complex and other Fe^{III}−heme−thiolate proteins are higher than the association rate constants known for NO binding to imidazole-ligated Fe^{III}−heme proteins and equal to or slightly lower than rates common to many ferrous heme proteins (see Table 4). However, there is no dramatic difference in these values, as expected. Taking into account that the heme proteins even with the same proximal ligand (imidazole or thiolate) exhibit quite a wide range of binding rate constants for NO, it is difficult to predict what the real effect of an axial thiolate ligand on the reactivity of iron porphyrin and its ligand substitution behavior would be. As already mentioned, the dynamics of NO binding to the heme proteins is affected to a large extent by the protein structure and the accessibility of the heme binding pocket. The lower NO binding rate constants suggest that the heme proteins possess substantial steric hindrance to ligand binding, or there is a need to replace a sixth ligand occupying the binding site (for example, as in the case of NO binding to the substrate-free and camphor-bound forms of $P450_{cam}$[25]). Comparison of the association rate constants obtained in the present study for the model SR complex with those found for the other model iron(III) porphyrins, Fe^{III}(TPPS) and Fe^{III}(TMPS)[35−37] (Table 4), demonstrates that in the present case, thiolate ligation of the iron(III) center appears to have only a minor, if any, influence on the

Table 3. Rate Constants k_{on} and k_{off} for the Nitrosylation of Ferriheme−Thiolate Proteins

ferric proteins[a]	k_{on} ($M^{-1}\ s^{-1}$)	k_{off} (s^{-1})	conditions	ref
eNOS[b]	6.1×10^5	93	at 10 °C, pH = 7.4, stopped-flow kinetic, k_{off} determined	39
eNOS[c]	8.2×10^5	70	from the intercept of the plot k_{obs} vs [NO]	
eNOS[d]	2.8×10^5	100		
nNOS[e]	1.9×10^7	50	at 23 °C, Tris buffer, pH 7.8, laser flash photolysis; k_{off} determined from the intercept of the plot k_{obs} vs [NO]	38
nNOS[f]	6.1×10^6	60	conditions as above but k_{off} determined by NO-trapping method using MbO_2 as NO scavenger	
nNOS[e]		5		
nNOS[f]		2		
$P450_{nor}$	1.9×10^7		at 20 °C, sodium phosphate buffer, pH = 7.2, laser flash photolysis	23
$P450_{cam}$	3.2×10^5	0.35	at 25 °C, K−phosphate buffer, pH = 7.4, substrate-free $P450_{cam}$	25
	3.4×10^6	1.9	at 25 °C, K−phosphate buffer, pH = 7.4, camphor-bound $P450_{cam}$	25

[a] Abbreviations: eNOS = endothelial nitric oxide synthase; nNOS = neuronal nitric oxide synthase; $P450_{nor}$ = nitric oxide reductase; $P450_{cam}$ = cytochrome P450, enzyme in the hydroxylation of camphor; H4B = (6*R*)-5,6,7,8-tetrahydro-L-biopterin. [b] H4B-saturated eNOS in the absence of the substrate. [c] H4B-saturated eNOS in the presence of arginine. [d] H4B-saturated eNOS in the presence of N^{ω}-hydroxy-L-arginine (NOHA). [e] Heme domain in the presence of H4B. [f] Holoenzyme in the presence of H4B.

(35) Ford, P. C.; Lorković, I. M. *Chem. Rev.* **2002**, *102*, 993.
(36) Hoshino, M.; Ozawa, K.; Seki, H.; Ford, P. C. *J. Am. Chem. Soc.* **1993**, *115*, 9568.
(37) Laverman, L. E.; Ford, P. C. *J. Am. Chem. Soc.* **2001**, *123*, 11614.

Table 4. Binding and Dissociation Rate Constants for the Reaction of Nitric Oxide with Representative Hemoproteins and Model Iron(II/III) Porphyrins (adopted from ref 40)

	conditions	k_{on} (M^{-1} s^{-1})	k_{off} (s^{-1})	K (M^{-1})	ref
		iron(II)			
Mb^{II}	phosphate buffer, pH 7.0	1.7×10^7	1.2×10^{-4}	1.4×10^{11}	41
Hb^{II}	phosphate buffer, pH 7.0	2.5×10^7	4.6×10^{-5}	5.3×10^{11}	41
Cyt c^{II}	H_2O	8.3	2.9×10^{-5}	2.9×10^5	36
cytochrome oxidase	pH 7.0	1×10^8	1.2×10^{-2}	8.3×10^9	42
guanylate cyclase	PH 7.0	7×10^8	7×10^{-4}	1.0×10^{12}	43, 44
Fe^{II} (TPPS)	H_2O, pH 6.5	1.8×10^9	~0	$>10^9$	37
Fe^{II} (TMPS)	pH 7.0	1×10^9			37
		iron(III)			
Mb^{III}	H_2O, pH 6.5	1.9×10^5	13.6	1.4×10^4	36
	Tris buffer, pH 7.4	2.71×10^4	16.0	1.7×10^3	27
Hb^{III}		4×10^3	1	4×10^3	45
Cyt c^{III}	H_2O, pH 6.5	7.2×10^2	4.4×10^{-2}	1.6×10^4	36
microperoxidase		1.1×10^6	3.4	3.2×10^5	46
Fe^{III} (TPPS)	H_2O, pH 6.5	7.2×10^5	6.8×10^2	1.1×10^3	36
Fe^{III} (TMPS)	H_2O pH 6.0	3×10^6	7.3×10^2	4.1×10^3	36

rate of the nitrosylation reactions, or this effect is covered by the different labilities of the leaving groups (viz. methanol and water for the SR and Fe^{III}(porph) complexes, respectively). The almost 3 orders of magnitude difference in association rate constants for the studied SR complex and model iron(II) porphyrins (Fe^{II}(TPPS) and Fe^{II}(TMPS)[35−37]) with NO is not surprising and is also seen for the nonthiolate-ligated iron porphyrins.

The value of the dissociation rate constant for the SR(NO) complex, determined from the intercept of the k_{obs} versus [NO] plot in the stopped-flow studies, is $k_{off}^{(1)} = 1.8 \pm 2.1$ s^{-1} at 5 °C. It is subjected to a large extrapolation error, but direct measurements of the reverse reaction with $Ru^{III}(edta)H_2O^-$ as a trapping agent for NO were hampered by the occurrence of subsequent multiphase reactions. NO dissociation rate constants found from NO-trapping experiments for the neuronal nitric oxide synthase and $P450_{cam}$ enzymes differ but not that substantially from the value calculated in the present study.[25,38] However, the NO dissociation rates for the nNOS enzymes measured by extrapolation of the complex formation kinetics (flash photolysis studies) were found to be ca. 10−20 times higher (see Table 3).

The overall equilibrium constant for the reaction between NO and the SR(Fe^{III}) complex (eq 1) calculated from the kinetic data (k_{on}/k_{off}) is $K_{NO} = (1.2 \pm 1.4) \times 10^5$ M^{-1} in methanol solution at 5 °C. It is somewhat higher than the value of K_{NO} reported in an earlier study[17] for the same reaction in CH_2Cl_2 solution (viz. $K_{NO} = 1.5 \times 10^5$ M^{-1} at 25 °C). Taking into account that NO binding rates for the SR complex in a noncoordinating solvent, such as CH_2Cl_2, should be even faster than those in methanol solution (since formation of the Fe−NO bond does not require displacement of a solvent molecule), it can be expected that the apparent lower stability of the SR(NO) complex in CH_2Cl_2 is the result of the high value of the dissociation rate constant for this complex in CH_2Cl_2 solution.

Suggested Mechanism for SR(NO) Complex Formation. The thermal activation parameters for the "on" reaction described by eq 1 show large and positive values of $\Delta H^{\ddagger}$ and $\Delta S^{\ddagger}$ (Table 1). They are accompanied by a positive activation volume, suggesting a dissociative ligand substitution mechanism that is dominated by the dissociation of the methanol molecule, according to Scheme 2.

Scheme 2

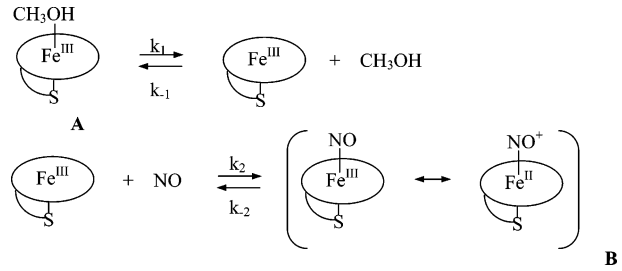

Application of the steady-state approximation to the unsaturated intermediate (five-coordinate SR molecule) results in the expression for k_{obs} given in eq 3.

$$k_{obs} = \frac{k_1 k_2[NO] + k_{-1}k_{-2}[CH_3OH]}{k_{-1}[CH_3OH] + k_2[NO]} \qquad (3)$$

Since k_{-1} and k_2 involve ligand binding to the unsaturated metal center and $[CH_3OH] \geq [NO]$, eq 3 takes the form $k_{obs} = k_{on}[NO] + k_{off}$, where $k_{on} = k_1k_2/k_{-1}[CH_3OH]$ and $k_{off} = k_{-2}$. Since k_{-1} and k_2 represent the binding of small, neutral molecules (CH_3OH or NO) to the unsaturated metal center, the difference in their activation parameters (i.e., $\Delta H_2^{\ddagger} - \Delta H_{-1}^{\ddagger}$, $\Delta S_2^{\ddagger} - \Delta S_{-1}^{\ddagger}$, and $\Delta V_2^{\ddagger} - \Delta V_{-1}^{\ddagger}$) should largely cancel out. For that reason, the on reaction is expected to be dominated by the k_1 pathway, which involves dissociation of CH_3OH and formation of the five-coordinate SR complex. As a result, the large and positive value of $\Delta H_{on}^{\ddagger(1)}$ found in this study for the forward reaction must reflect the energy required to break the $Fe^{III}-CH_3OH$ bond, while the sizable $\Delta S_{on}^{\ddagger(1)}$ value should be consistent with the formation of two molecules from one without any significant solvational changes. The positive value of $\Delta V_{on}^{\ddagger(1)}$ is also in good agreement with the reaction mechanism outlined in Scheme 2. However, it seems to be much smaller than that found recently[25] for the related reaction between NO and the thiolate-ligated iron(III) hemoprotein, cytochrome $P450_{cam}$. The value of $\Delta V_{on}^{\ddagger}$ for NO binding to the substrate-free cytochrome $P450_{cam}$ (low-spin, six-coordinate aqua complex) was reported to be $+28 \pm 2$ cm^3 mol^{-1}. This large value

(38) Scheele, J. S.; Bruner, E.; Kharitonov, V. G.; Martásek, P.; Roman, L. J.; Masters, B. S. S.; Sharma, V. S.; Magde, D. *J. Biol. Chem.* **1999**, *274*, 13105.

includes not only a volume increase due to $Fe^{III}-H_2O$ bond breakage but also a volume increase associated with the low-spin (aqua complex, $S = {}^1/_2$, doublet) to high-spin (five-coordinate, $P450_{cam}$ intermediate, $S = {}^5/_2$, sextet) transition.[25] In the present case, the k_1 pathway represents a reaction between two low-spin species ($S = {}^1/_2$), such that the volume change mainly involves $Fe^{III}-CH_3OH$ bond breakage. Furthermore, in the case of NO binding to cytochrome $P450_{cam}$, significant volume changes could also be associated with structural rearrangements of the protein pocket during formation of the five-coordinate intermediate. This effect is excluded in the case of NO binding to the model SR complex. A similar trend in the volume changes was observed for the reaction of NO with imidazole-ligated iron(III) hemoproteins and model iron(III) porphyrins. For example, NO binding to metmyoglobin is accompanied by an activation volume significantly larger ($\Delta V_{on}^{\ddagger} = +21 \pm 1$ cm^3 mol^{-1})[27] than that found for the model porphyrin system ($\Delta V_{on}^{\ddagger} = +8 \pm 1$ cm^3 mol^{-1}).[37]

The SR(NO) complex was found to be EPR-silent. However, it is difficult to distinguish which form of this complex is more likely, $Fe^{III}-NO^{\bullet}$ (spin pairing of $S = {}^1/_2$ (Fe^{III}) and $S = {}^1/_2$ (NO)) or $Fe^{II}-NO^+$ (binding of two diamagnetic molecules, Fe^{II} and NO^+). Resonance Raman and IR spectroscopy revealed that the ν(N−O) mode in the SR(NO) complex is fairly close in its nature to the ν(N−O) modes of other natural heme−thiolate-containing enzymes.[17] This could indicate that the Fe−NO group in the nitrosyl complex of SR also adopts a linear structure and an $Fe^{II}-NO^+$ character as it was observed, for example, for $P450_{cam}$(NO).[47] Hence, the k_2 pathway depicted in Scheme 2 should involve not only $Fe^{III}-NO$ bond formation but also considerable charge transfer from NO to the iron(III) atom to formally give the $Fe^{II}-NO^+$ species. During this bond formation process, the spin state of iron changes from $S = {}^1/_2$ (low-spin, doublet) to $S = 0$ (low-spin, singlet).

Unfortunately, the determination of activation parameters for the release of NO from SR(NO) was complicated by the occurrence of the subsequent multiphase reactions. However, in terms of microscopic reversibility, the reverse process (k_{off} pathway) must proceed via the same intermediates as those generated during the k_{on} pathway. If so, it is reasonable to expect that the "off" reaction also follows a limiting dissociative mechanism for which the k_{-2} pathway seems to be the energetically dominant step. Thus, the activation parameters for the off reaction should, in principle, reflect the intrinsic entropy and volume changes associated with breakage of the Fe−NO bond, a spin change from $S = 0$ to $S = {}^1/_2$, a formal oxidation of Fe^{II} to Fe^{III}, and solvent reorganization if the nitrosyl complex of SR has an $Fe^{II}-NO^+$ character.

Scheme 3

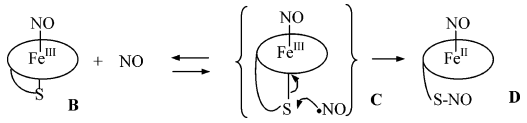

Explanation Offered for the Subsequent Thermal Reactions. The second reaction step was shown to be nearly 10 times slower than the formation of SR(NO). The reverse reaction is close to zero within the experimental error limits. The substantially negative values found for the activation entropy and activation volume (viz. -87 ± 6 J mol^{-1} K^{-1} and -16.3 ± 0.8 cm^3 mol^{-1}, respectively) clearly support an associative mechanism. In principle, two possible explanations can be offered to account for these features. One involves the attack of a second NO molecule on the initially formed $Fe^{III}-NO$ species, leading to the formation of an N−N coupled intermediate followed by a metal-assisted NO disproportionation reaction. Similar $(NO)_2$ adducts were proposed earlier for the reactions of NO with iron(II) porphyrins[48] and heme-based NOR enzymes.[20b,23,49] It was shown that the NO disproportionation ability of nitrosyl complexes depends on the anionic character of the coordinated nitrosyl ligand[50] and is strongly inhibited by protic solvents.[48] However, several lines of evidence sharply contrast these observations and indicate that nitrosyl iron porphyrins do not react with an excess of NO at room temperature, and formation of such $(NO)_2$ intermediates is rather hampered.[51] Regardless of this issue, taking into account that in the present study, the nitrosylation reaction was carried out in a protic solvent and NO binding to the SR complex may be accompanied by charge transfer from NO to Fe(III) to formally give $Fe^{II}-NO^+$ species, formation of such a N−N coupled intermediate in the studied SR/NO system should rather be excluded.

A markedly different pathway providing a more reasonable explanation for the kinetic data found for the second reaction would be the direct attack of the second NO molecule on the sulfur atom of the thiolate ligand in the initially formed nitrosylated SR complex (**B**), according to Scheme 3. Although the thiolate ligand in the SR complex is sterically protected by bulky groups, formation of the S-nitrosylated derivative (**C**) under conditions of a large excess of NO does not seem unusual. A similar scenario was observed for the reaction between nitric oxide and the stable thiolatocobalamin (i.e., glutathionylcobalamin).[52] Kinetic studies on this reaction indicated the formation of the intermediate (Cbl(II) + *S*-nitrosoglutathione) cage, with the second-order rate constant, $k_{on} = 2.82 \times 10^3$ M^{-1} s^{-1}, followed by the fast reaction of Cbl(II) with NO to form Cbl(II)−NO as the final product. Moreover, very recent studies[53] on the nitric oxide interaction with insect nitrophorins (NO-carrying heme proteins found in blood-sucking insects) have revealed that these thiolate-ligated iron(III) hemoproteins are able to bind two molecules of NO, one to the heme in the distal

(39) Abu-Soud, H. M.; Ichimori, K.; Presta, A.; Stuehr, D. J. *J. Biol. Chem.* **2000**, *275*, 17349.
(40) Wanat, A.; Wolak, M.; Orzel, L.; Brindell, M.; van Eldik, R.; Stochel, G. *Coord. Chem. Rev.* **2002**, *229*, 37.
(41) Moore, E. G.; Gibson, Q. H. *J. Biol. Chem.* **1976**, *251*, 2788.
(42) (a) Giuffre, A.; Sarti, P.; D'Itri, E.; Buse, G.; Soulimane, T.; Brunori, M. *J. Biol. Chem.* **1996**, *271*, 33404. (b) Sarti, P.; Giuffre, A.; Forte, E.; Manstronicola, D.; Barone, M. C.; Brunori, M. *Biochem. Biophys. Res. Commun.* **2000**, *274*, 183.
(43) Kharitonov, V. G.; Russwurm, M.; Magde, D.; Sharma, V. S.; Koesling, D. *Biochem. Biophys. Res. Commun.* **1997**, *239*, 284.
(44) Stone, J. R.; Marletta, M. A. *Biochemistry* **1996**, *35*, 1093.
(45) Sharma, V. S.; Traylor, T. G.; Gardiner, R.; Mizukami, H. *Biochemistry* **1987**, *26*, 3837.
(46) Sharma, V. S.; Isaacson, R. A.; John, M. E.; Waterman, M. R.; Chevion, M. *Biochemistry* **1983**, *22*, 3897.
(47) Hu, S.; Kincaid, J. R. *J. Am. Chem. Soc.* **1991**, *113*, 2843.
(48) Lin, R.; Farmer, P. J. *J. Am. Chem. Soc.* **2001**, *123*, 1143.
(49) MacNeil, J. H.; Berseth, P. A.; Bruner, E. L.; Perkins, T. L.; Wadia, Y.; Westwood, G.; Trogler, W. C. *J. Am. Chem. Soc.* **1997**, *119*, 1668.
(50) Franz, K. J.; Lippard, S. J. *J. Am. Chem. Soc.* **1999**, *121*, 10504.
(51) (a) Lorković, I. M.; Ford, P. C. *Inorg. Chem.* **2000**, *39*, 632. (b) Lim, M. D.; Lorković, I. M.; Wedeking, K.; Zanella, A. W.; Works, C. F.; Massick, S. M.; Ford, P. C. *J. Am. Chem. Soc.* **2002**, *124*, 9737.
(52) Zheng, D.; Birke, R. L. *J. Am. Chem. Soc.* **2002**, *124*, 9066.
(53) (a) Walker, F. A. *J. Inorg. Biochem.* **2005**, *99*, 216. (b) Weichsel, A.; Maes, E. M.; Andersen, J. F.; Valenzuela, J. G.; Shokhireva, T. Kh.; Walker, F. A.; Montfort, W. R. *Proc. Natl. Acad. Sci. U.S.A.* (submitted).

Scheme 4

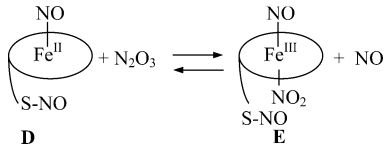

pocket and the other to the cysteine thiolate ligand to produce an *S*-nitrosyl (SNO) conjugate. The formation of the Cys−SNO moiety was confirmed by structural investigations of the crystals of this protein after treatment with nitric oxide, as well as by EPR studies, which clearly indicate the formation of an EPR-active Fe(II)−NO complex after homolytic cleavage of the Fe(III)−S−Cys bond.[53b]

Suzuki and co-workers[17] demonstrated for benzene solutions of SR that the reaction with an equivalent amount of NO is completely reversible and does not lead to nitrosylation of the thiolate group. However, EPR measurements in this study indicated that the addition of a small excess of nitric oxide resulted in the formation of a new EPR-active, five-coordinate Fe^{II}−heme−NO complex. The N−O stretching mode found for this complex by IR spectroscopy is characteristic for the other known Fe^{II}−porphyrin−NO systems.[32] This can suggest that under conditions of an excess of NO, attack of the NO molecule on the thiolate ligand is accompanied by the homolytic cleavage of the Fe−S bond, which leads to the formation of the five-coordinate SR(Fe^{II}) nitrosyl complex (**D**). Alternatively, thiyl radical formation followed by radical−radical coupling with the NO radical could also account for the process from **B** to **D** in Scheme 3. In principle, two distinct ν(N−O) stretching modes for the Fe−(NO) and S−(NO) groups are expected for complex **D**. However, since a strong IR band at about 1500 cm^{-1} was observed for the SR complex,[14] it is likely that ν(N−O) for the S−(NO) group is hidden under this band.

Decomposition of species **D** is *strongly* accelerated by the presence of a large excess of nitric oxide. It seems that attack of a second NO molecule on the vacant site of the five-coordinate SR(Fe^{II}) species can be excluded under such conditions. As demonstrated by Ford et al.[51] for ambient temperature conditions, the formation of dinitrosyl iron(II) porphyrin complexes is relatively weak ($K < 3\ M^{-1}$ at 25 °C), with the result that such complexes can only be observed at lower temperatures. These observations lead to the conclusion that the subsequent reaction step characterized by the slow absorbance decrease at 416 nm with concomitant appearance of the shoulder at 430 nm can be due to the attack of N_2O_3 on the five-coordinate SR(Fe^{II}) center to give a nitrosyl−nitrite complex, as shown in Scheme 4. Acceleration of this reaction under conditions of a large excess of nitric oxide can be explained in terms of the presence of the higher nitrogen oxides (N_2O_3) present as impurities in the saturated NO solutions[33b,51] (as the result of NO oxidation by trace quantities of oxygen: $2NO + O_2 \rightarrow 2NO_2$ and $NO_2 + NO \rightarrow N_2O_3$; or the presence of NO_x in the source of NO). Our own experience,[33a] as well as those of other groups,[33b−d,51] has clearly shown that it is practically impossible to prevent the formation of N_2O_3 under such experimental conditions, that is, in saturated NO solutions. Thus, experiments in the absence of N_2O_3 under such conditions cannot be performed in order to directly prove the suggested reaction sequence.

The validity of the above proposed reaction can, however, be easily checked in an indirect way by introducing a small quantity of oxygen to the SR/NO system (oxidation of NO to NO_2 and to N_2O_3 under an excess of NO). This led to the rapid formation of a species with a maximum band at 430 nm. It should be noted that in experiments with an excess of NO (when all possible efforts were undertaken to remove O_2 from the SR/NO system), this band was only observed as a weak shoulder due to the low N_2O_3 concentration present. The electronic spectrum of the new complex resembles spectra of other $Fe^{III}(NO)(NO_2)$ porphyrin complexes which are structurally and spectrally well characterized in the literature.[51,54] IR spectra of a chloroform solution of SR recorded under a large excess of NO are also in good agreement with these observations. The nitrosyl stretching frequency found for the SR(Fe^{III})(NO)(NO_2) species (1891 cm^{-1}) is consistent with that observed previously (1871−1893 cm^{-1})[54c] for the similar Fe^{III}(porph)(NO)(NO_2) systems (where porph = TPP, OEP, T*p*-OCH_3PP, and TpivPP). However, it should be mentioned that the IR band at 1891 cm^{-1} with an isotope shift of about 36 cm^{-1} is characteristic for the N−O stretching vibration of coordinated NO^+ (the position and ^{15}N isotope shift are identical with those of the complexes containing linear M−NO^+ units). Hence, the nitro−nitrosyl complex of SR can be formally assigned as the SR(Fe^{II})(NO^+)(NO_2) species.

The other band observed at 1301 cm^{-1} with a ^{15}N isotope shift of about 20 cm^{-1} is consistent with that characteristic of nitro complexes[54d] and can be assigned to the $\nu_s(NO_2)$ mode. The antisymmetric stretching mode of the nitro ligand, $\nu_a(NO_2)$, is expected at about 1440 (1460) cm^{-1}. However, since the SR complex itself shows a band at 1447 cm^{-1},[14] the antisymmetric stretching mode of the NO_2 group cannot be clearly observed in the FTIR spectrum of the SR(Fe^{II})(NO^+)(NO_2) species.

Fe^{III}(porph)(NO)(NO_2) complexes were demonstrated to be relatively stable under high [NO] and well defined [N_2O_3] conditions.[51] Equilibrium constants for the reaction between N_2O_3 and various Fe^{II}(porph) complexes were estimated to range from 1.0 to 400, depending on the electron-donating properties of the porphyrins.[54e] In the present study, the concentration of N_2O_3 under conditions of a large excess of NO is expected to be not so high. Thus, it is assumed that the equilibrium of the reaction depicted in Scheme 4 can be shifted to the five-coordinate nitrosyl SR(Fe^{II}) species (complex **D**). Moreover, the formation of the stable SR(Fe^{II})(NO^+)(NO_2) complex in the investigated system seems to be rather impossible under the applied conditions with methanol as a solvent. It has already been reported that methanol can be involved in the facile nucleophilic attack at coordinated nitrosyl (NO^+) and lead to the reductive nitrosylation of the ferric porphyrins.[34] Furthermore, nitrite ion present as impurity in NO solutions has also been shown to catalyze the reductive nitrosylation of ferriheme systems[55a] and their water-soluble porphyrin models.[55b,c] Notably, addition of nitrite to the SR/NO system significantly

(54) (a) Settin, M. F.; Fanning, J. C. *Inorg. Chem.* **1988**, *27*, 1431. (b) Yoshimura, T. *Inorg. Chim. Acta* **1984**, *83*, 17. (c) Ellison, M. K.; Schulz, C. E.; Scheidt, W. R. *Inorg. Chem.* **1999**, *38*, 100. (d) Nakamoto, K. *Infrared and Raman Spectra of Inorganic and Coordination Compounds*, 3rd ed.; Wiley-Interscience: New York, 1978. (e) Lorković, I. M.; Lim, M. D.; Wedeking, K.; Ford, P. C. Manuscript in preparation.

(55) (a) Fernandez, B. O.; Ford, P. C. *J. Am. Chem. Soc*. **2003**, *125*, 10510. (b) Fernandez, B. O.; Lorković, I. M.; Ford, P. C. *Inorg. Chem*. **2003**, *42*, 2. (c) Fernandez, B. O.; Lorković, I. M.; Ford, P. C. *Inorg. Chem*. **2004**, *43*, 5393.

Scheme 5

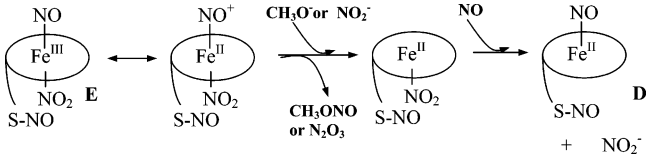

accelerated the final reaction step characterized by the absorbance increase at 416 nm and decrease at 430 nm. All of these observations lead to the conclusion that the final and slowest reaction most likely represents the reductive nitrosylation of the $SR(Fe^{II})(NO^+)(NO_2)$ complex to $SR(Fe^{II})(NO)$ species in the presence of nucleophiles, such as CH_3O^- or NO_2^- (formed in small amounts in NO-saturated methanol solutions), according to Scheme 5. This is also confirmed by the electronic spectrum of the final complex, which resembles the spectrum of complex **D** (a Soret band at 416 nm).

The multiple reaction steps studied in the present system can be regarded as a good model for the reactions occurring under aerobic conditions. As it was demonstrated for the SR/NO system, the presence of even a small amount of oxygen as impurity can lead to the subsequent reactions in which dynamic equilibria involving reactive SR species and higher nitrogen oxides NO_x (free or coordinated) seem to play an important role. It is supposed that a similar scenario can also occur in vivo under aerobic conditions, that is, NO_x can either coordinate to the metal center (as in Scheme 4) or act as a nucleophile (catalyst) leading to the reductive nitrosylation of the ferriheme proteins (as in Scheme 5).

Reaction Product of NO_2^- Binding to $SR(Fe^{III})$. Treatment of the SR complex with only nitrite results in a reaction product with a spectrum very similar to that recorded for the reaction with a large excess of NO. However, the reaction pathway leading to this final species is *much longer* than that in the case of the reaction with NO and involves many steps. Similar reactions in the nitrite/iron(III) porphyrinate systems have already been investigated by Scheidt and co-workers.[56] All observations are consistent with an instability of such systems, which leads not to the expected nitrite-coordinated species but rather to the formation of iron(II) nitrosyl complexes.[56a] This unique instability of the nitrite complexes of iron(III) porphyrins is ascribed to oxygen atom transfer from iron-bound nitrite to a variety of substrates, including NO_2^-. Only reactions of nitrite with (porphyrinato)iron(III) complexes having a special protected ligand-binding site result in the desired nitrite complexes.[56b,c] On the basis of these findings, we can conclude that in the studied SR/NO_2^- system, the final reaction product should not be a nitrite-coordinated $SR(Fe^{III})$ complex but rather a nitrosyl $SR(Fe^{II})$ species. Since the reaction of SR with a large excess of NO also gives the nitrosyl adduct of the reduced SR complex as a final reaction product, this can explain why in both studied processes, the spectra of the final species are very similar.

Possible Scenario for the Reactions Generated by Laser Flash Photolysis. Since all flash photolysis experiments were carried out in methanol under conditions of a large excess of NO, the main species present in the solutions subjected to flash

(56) (a) Finnegan, M. G.; Lappin, A. G.; Scheidt, W. R. *Inorg. Chem.* **1990**, *29*, 181. (b) Nasri, H.; Goodwin, J. A.; Scheidt, W. R. *Inorg. Chem.* **1990**, *29*, 185. (c) Nasri, H.; Haller, K. J.; Wang, Y.; Huynh, B. H.; Scheidt, W. R. *Inorg. Chem.* **1992**, *31*, 3459.

Scheme 6

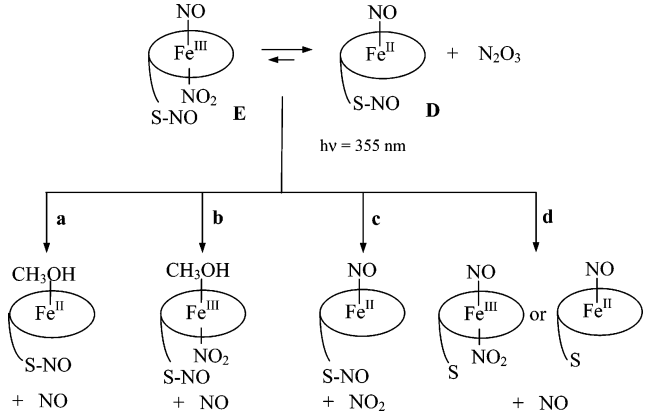

excitation at 355 nm was not $SR(Fe^{III})(NO)$ (**B**), as initially expected, but an equilibrium of $SR(Fe^{II})(NO)$ (**D**) and $SR(Fe^{III})(NO)(NO_2)$ (**E**), with the former in excess. It should be also noted that complex **E** underwent reductive nitrosylation in methanol solution during the flash photolysis measurements, thus it is very difficult to predict the ratio of [**D**]/[**E**] for each performed experiment. This finding enabled us to clarify the results obtained from the flash photolysis studies. In summary, difference transient spectra and kinetic traces recorded at a single wavelength following flash photolysis of the SR/NO solution clearly indicated multiple processes, that is, one reaction occurring on the microsecond time scale with a transient absorption centered at 428 nm and two reactions on the millisecond time scale with a transient absorption at 420 nm. A *possible* mechanism providing a reasonable explanation for the observed reactions and photoproducts generated by flash photolysis is illustrated in Scheme 6.

In this scheme, the formation of photoproduced intermediates may occur, in principle, along four pathways (**a**−**d**). One of these (pathway **a**) involves photodissociation of NO from complex **D** to give a S-nitrosylated $SR(Fe^{II})$ intermediate (transient difference spectrum with a positive peak at 428 nm) which reacts rapidly with excess NO ($k_a = (1.21 \pm 0.03) \times 10^8$ M^{-1} s^{-1} at 25 °C) to regenerate the starting complex. It should be noted that the spectrum observed 14.6 μs after the flash with a maximum at 428 nm resembles the difference spectrum obtained by subtracting the spectrum of $SR(Fe^{II})(NO)$ (or S-nitrosylated $SR(Fe^{II})(NO)$) from that of $SR(Fe^{II})$. The latter two spectra were prepared by exposure of a degassed methanol solution of $SR(Fe^{II})$, produced by chemical reduction with $NaBH_4$/18-crown-6, to NO. The value of the second-order rate constant (k_a) found for the reaction between NO and the five-coordinate $SR(Fe^{II})$ complex is about 2 orders of magnitude higher than that obtained for NO binding to the oxidized $SR(Fe^{III})$ complex (see Scheme 2).

A second, competitive pathway (**b**) involves photodissociation of NO from complex **E**, leading to the formation of the $SR(Fe^{III})(NO_2)$ intermediate. The latter reacts with the excess of NO much slower than it was observed for pathway **a**, for which the second-order rate constant was $k_b = (4.09 \pm 0.08) \times 10^4$ M^{-1} s^{-1} at 25 °C. This value is 1 order of magnitude smaller than that found for the relevant reaction between $Fe^{III}(TPP)(NO_2)$ and nitric oxide studied in toluene solution.[54d] The higher value of the rate constant for the binding of NO found for the latter complex could indicate that in this case,

NO binds to the unsaturated five-coordinate Fe^{III} center (in a noncoordinating solvent) and does not require displacement of a methanol molecule.

The third pathway (**c**) shown in Scheme 6 suggests the possibility that NO_2 (as radical) in complex **E** is photolabilized, and a five-coordinate iron(II) intermediate can be formed. Detection at a single wavelength on a longer time scale revealed that the photoproduct in this reaction decays slowly and finally leads to the full regeneration of the initial spectrum. However, as a result of *very small* absorbance changes, the third (and slowest) reaction observed following flash excitation was not studied in any further detail.

A fourth pathway (**d**) involves photodissociation of NO from the nitrosothiolate group of complex **D** or **E**. The thionyl radicals formed in this process will react very rapidly with nitric oxide via radical−radical coupling (almost diffusion controlled) to regenerate the starting complexes. However, it is assumed that under the selected applied experimental conditions (detection in the Soret region and low concentrations of **D** and **E**), spectrophotometric monitoring of such radical processes seems to be rather impossible.

As already noted, the reaction of SR(Fe^{III}) with NO_2^- does not lead to the desired nitrite-coordinated SR(Fe^{III}) complex, but to the nitrosyl SR(Fe^{II}) species. Thus, laser flash photolysis of the SR/NO_2^- system should not involve a simple nitrite photolabilization reaction from the SR(NO_2^-) complex, but rather represent photodissociation of NO from SR(Fe^{II})(NO). Transient difference spectra recorded for the SR/NO_2^- system are consistent with these expectations. They are very similar but not identical to the TRO spectra observed for the binding of NO to the S-nitrosylated SR(Fe^{II}) species immediately after flash photolysis of complex **D** (pathway **a**, Scheme 6). Photoinduced absorption changes for the solution of the SR complex with nitrite decay back to values close to zero on a substantially longer time scale (ca. 2 ms) than was observed for the reaction described by pathway **a** (ca. 0.3 ms). However, it should be noted that in pathway **a**, NO is used in a large excess, whereas in the SR/NO_2^- system, NO is generated in an equivalent amount (1:1) following flash excitation of the nitrosyl SR(Fe^{II}) complex.

Reaction of the SR Complex with NO in Toluene Solution. The absorption spectrum of the SR complex in toluene appears to be almost the same as that measured by Suzuki and co-workers in benzene solution[17] and is clearly distinguishable from that obtained in a polar solvent, such as methanol. As reported,[17] addition of a small quantity of NO to a degassed benzene solution of SR results in the *reversible* coordination of NO to the Fe^{III} center of the SR complex (without modification of the thiolate group) to form the SR(NO) complex that displays the Soret and Q-bands at 439 and 555 nm, respectively. However, experiments carried out in toluene under conditions of an excess of NO revealed that even in nonpolar solvents, interaction of SR with NO involves subsequent reaction steps, as it was observed in methanol solution. The first fast reaction observed on stopped-flow mixing of SR in toluene with an excess of NO at −50 °C is ascribed to the formation of SR(NO). It is characterized by a Soret band shift from 411 to 439 nm and leads to a spectrum that is very similar to that obtained for the SR(NO) complex in benzene solution. The second-order rate constant for the formation of SR(NO), $k^{(1)}_{(tol)} = (6.9 \pm 0.6) \times 10^4\ M^{-1}\ s^{-1}$ at −50 °C, is almost 3 orders of magnitude higher than that found for the formation of SR(NO) in methanol, $k_{on}^{(1)} \approx 73\ M^{-1}\ s^{-1}$ at −50 °C (calculated from the temperature dependence of $k_{on}^{(1)}$). This finding illustrates once again how important the accessibility of the metal center is for the binding of NO. The formation of SR(NO) in methanol requires initial displacement of coordinated methanol, in contrast to the binding of NO to the five-coordinate Fe(III) center observed in experiments performed in noncoordinating toluene or to the five-coordinate SR(Fe^{II}) intermediate produced after laser flash excitation (see discussion above).

As in the case of methanol as solvent, under conditions of a large excess of NO, the formation of SR(NO) in toluene is also followed by a subsequent, slower reaction which is accompanied by the appearance of a new band maximum at 425 nm. The second-order rate constant found for this reaction, $k_{(tol)}^{(2)} = (2.5 \pm 1.0) \times 10^3\ M^{-1}\ s^{-1}$ at −50 °C, is within experimental error very close to that found for the second reaction step, $k_{on}^{(2)} = (2.1 \pm 0.2) \times 10^3\ M^{-1}\ s^{-1}$ at −50 °C (Table 1). For this reason, it is suggested that the second reaction step observed in toluene under conditions of a large excess of NO may also involve direct attack of the second NO molecule on the sulfur atom of the thiolate ligand in the initially formed nitrosylated SR complex, as it was observed in experiments carried out in methanol.

The subsequent, slower reaction(s) leading to the final product with a Soret band at 433 nm was not the subject of further study. However, it is reasonable to expect that this slow process presumably involves attack of higher nitrogen oxides (NO_x) on the reactive SR(Fe^{II}) species leading to the formation of the nitrosyl−nitrite complex of SR(Fe^{III}), as observed in the case of the reaction of the SR complex with a large excess of NO in methanol solution.

Conclusions

Under the condition of low NO concentrations, the synthetic heme−thiolate SR complex reversibly binds NO. The second-order rate constants determined for the SR(NO) complex formation reaction in polar and nonpolar solvents indicate that the complex can be regarded as a good model for the kinetics of the analogous reactions with Fe^{III}−heme−thiolate proteins. Experiments carried out in methanol and toluene solutions demonstrate that the NO binding dynamics is governed by the coordination mode of the iron center. The activation parameters found for the formation of SR(NO) in methanol indicate a limiting dissociative mechanism that is dominated by the dissociation of coordinated methanol. In contrast, binding of NO to SR in a noncoordinating solution, such as toluene, does not require displacement of coordinated solvent and occurs almost 3 orders of magnitude faster than in methanol solution. A similar scenario was observed for the binding of NO to ferric $P450_{cam}$ in the absence and presence of camphor as substrate. However, as we discussed in our previous paper,[25] in this case, two opposite effects (i.e., facilitation of NO binding due to a vacant coordination site and slowing down the binding rate due to rigidity of the active site) seem to play important roles. The reactivity of $P450_{nor}$ or NOS enzymes toward NO is much higher compared with that of $P450_{cam}$. Since the heme coordination structure of the iron center of $P450_{nor}$ is similar to that of the substrate-free form of $P450_{cam}$[21] (a water molecule occupies the

sixth coordination site of the heme iron and the same effect of electron donation from S^-), the difference in the catalytic property of these enzymes cannot be explained in terms of the difference in the nature of their iron centers. In this case, the reaction dynamics of NO binding seems to be far more dominated by steric and/or electrostatic effects of the protein environment in the heme binding pocket. Indeed, the study on the binding of CO to the reduced forms of $P450_{cam}$ and $P450_{nor}$[23b] also confirmed that the heme pocket of the latter must be sterically less hindered toward the external ligand (or larger in size) than that of $P450_{cam}$. Moreover, the proximal and distal heme environments appear to play a crucial role in controlling the iron spin state (the presence of the proximal ligand or its absence) as well as in stabilizing thiolate coordination to the iron heme centers.[57] The importance of the protein structure in the neighborhood of the iron center can be reflected by the comparison of the NO binding kinetics observed for the Fe^{III}–heme–thiolate proteins with that of their protein-free model complex (viz. SR complex). It seems very likely that the role of the protein pocket is to *regulate* (facilitate or slow) the rates of NO binding or release processes, depending on the physiological requirements. The simultaneous interplay of the effects coming from the protein environment of the heme pocket and from the coordination mode of the iron(III) center (vacant coordination site or the lability of the leaving group) makes the quantification of the real trans effect of the proximal thiolate coordination in such systems more problematic.

Under conditions of an excess of NO, rapid formation of SR(NO) is followed by subsequent reactions. They can be explained in terms of direct attack of a second NO molecule on the thiolate ligand in the initially formed SR(NO) complex or can involve dynamic equilibria between higher nitrogen oxides and reactive SR species, which lead to the formation of the nitrosyl–nitrite $SR(Fe^{II})$ complex as the final product. It should be noted that in biological systems, the concentration of NO is *much* lower than that employed in our experiments with the model SR complex. Thus, under physiological conditions, direct attack of a second NO molecule on the sulfur atom coordinated to the Fe(III) heme center and well protected by the protein pocket should be rather excluded. This is also confirmed by our recent studies on NO binding to cytochrome $P450_{cam}$,[25] in which the use of NO even in a large excess did not lead to nitrosylation of the proximal thiolate group of cyt $P450_{cam}$. However, the recent study[53] on the NO binding to the *Cimex* nitrophorin revealed that interaction of the nitric oxide with the naturally occurring thiolate-ligated Fe(III)heme proteins can lead to the formation of such a Cys–S(NO) moiety. On the other hand, redox-related NO_x species will always exist under aerobic physiological conditions, from which it follows that on the basis of the results presented here, clarification of the potential role of higher nitrogen oxides in the chemistry of transition metal complexes could be helpful for understanding the molecular mechanisms operating in biological transformations.

(57) Roach, M. P.; Pond, A. E.; Thomas, M. R.; Boxer, S. G.; Dawson, J. H. *J. Am. Chem. Soc.* **1999**, *121*, 12088.

Acknowledgment. The authors gratefully acknowledge financial support from the Deutsche Forschungsgemeinschaft within SPP 1118. Studies at the Jagiellonian University were supported by the State Committee for Scientific Research, Poland, KBN (3T09A11515) and the Foundation for Polish Science ("Fastkin" No. 8/97). They also kindly acknowledge assistance from Thorsten Schneppensieper and Markus Weitzer (University of Erlangen-Nürnberg) and Andrzej Karocki (Jagiellonian University) with preliminary measurements during the earlier stage of the project.

Supporting Information Available: Temperature and pressure dependence for the formation of the SR(NO) complex (S1); spectral changes and typical absorbance–time plots for the subsequent reactions of the SR complex with NO measured with the stopped-flow instrument (S2); spectral changes and typical absorbance–time plots for the reaction of the SR complex with NO_2^- measured with the stopped-flow instrument (S3); kinetic traces and NO concentration dependence of k_{obs} observed during the laser flash photolysis of the SR/NO system (S4 and S5); transient absorption difference spectra recorded for the SR complex following laser flash photolysis (S6); and spectral changes for the second reaction of the SR complex with a large excess of NO in toluene solution, typical absorbance–time plot recorded for the first reaction during SR(NO) formation in toluene solution (S7). This material is available free of charge via the Internet at http://pubs.acs.org.

JA047572U